

Document downloaded from:

<http://hdl.handle.net/10251/160587>

This paper must be cited as:

Ortiz-Ramirez, CI.; Giraldo, MA.; Ferrandiz Maestre, C.; Pabon-Mora, N. (2019). Expression and function of the bHLH genes ALCATRAZ and SPATULA in selected Solanaceae species. *The Plant Journal*. 99(4):686-702. <https://doi.org/10.1111/tpj.14352>



The final publication is available at

<https://doi.org/10.1111/tpj.14352>

Copyright Blackwell Publishing

Additional Information

1 **Expression and function of the bHLH genes *ALCATRAZ* and *SPATULA* in selected**
2 **Solanaceae species**

3
4 **Clara Inés Ortiz-Ramírez**^{1,2}, **Marco A. Giraldo**³, **Cristina Ferrándiz**², **Natalia Pabón-**
5 **Mora**^{1,*}

6
7 ¹Instituto de Biología, Universidad de Antioquia, Medellín, Colombia, ²Instituto de Biología
8 Molecular y Celular de Plantas, Consejo Superior de Investigaciones Científicas–
9 Universidad Politécnica de Valencia, Valencia, Spain; ³Instituto de Física, Universidad de
10 Antioquia, Medellín, Colombia.

11
12 *Corresponding author:

13 Natalia Pabón- Mora

14 *Tel:* +57 3217720164

15 *Email:* lucia.pabon@udea.edu.co

16
17 *Running Title:* *The role of ALCATRAZ and SPATULA in Solanaceae*

18 **Keywords:** *ALCATRAZ*, berries, capsules, fruit development, lignification, pigmentation,
19 *SPATULA*, Solanaceae.

20
21 **Summary**

- 22 • The genetic mechanisms underlying fruit development have been identified in
23 Arabidopsis and have been comparatively studied in tomato as a representative of
24 fleshy fruits. However comparative expression and functional analyses on the bHLH
25 genes downstream the genetic network, *ALCATRAZ* (*ALC*) and *SPATULA* (*SPT*)
26 which are involved in the formation of the dehiscence zone in Arabidopsis, have not
27 been functionally studied in the Solanaceae.

- 28 • Here we perform detailed expression and functional studies of *ALC/SPT* homologs in
29 *Nicotiana obtusifolia* with capsules, and *Capsicum annuum* and *Solanum*
30 *lycopersicum* with berries.
- 31 • In Solanaceae, *ALC* and *SPT* genes are expressed in leaves, all floral organs,
32 especially in petal margins, stamens and carpels, however their expression changes
33 during fruit maturation according to the fruit type. Functional analyses show that
34 downregulation of *ALC/SPT* genes does not have an effect on gynoecium patterning,
35 however, they have acquired opposite roles in petal expansion and have been co-
36 opted in leaf pigmentation in Solanaceae. In addition, *ALC/SPT* genes repress
37 lignification in time and space during fruit development in Solanaceae.
- 38 • Altogether, some roles of *ALC* and *SPT* genes are different between Brassicaceae and
39 Solanaceae. In addition, the paralogs have undergone some subfunctionalization in
40 the former and are mostly redundant in the latter.

41

42

43

44 **Introduction**

45 Fruits are extreme ontogenetic transformations of the carpel walls as a result of ovule
46 fertilization (Esau 1967). As they are often fleshy, tasty and nutritious, fruits are at the core
47 of human and animal diets (Seymour *et al.*, 2013). However, not all fruits are fleshy and
48 frequently the carpel transforms into a pod that dries out and splits open to release the seeds
49 (Esau 1967). A fruit genetic regulatory network has been proposed for the development of
50 the siliques of the model *Arabidopsis thaliana*, based on loss- and gain-of-function mutants
51 that exhibit defects in fruit patterning and development, the identification of the
52 corresponding genes, and the characterization of their functional relationships by genetic
53 analyses (Dinneny *et al.*, 2005, Roeder & Yanofsky, 2006). The genetic model for fruit
54 development has served as reference for comparative studies in other model and non-model
55 plants. *Arabidopsis* species have siliques, which are dry dehiscent fruits formed by two fused
56 carpels. The ovary, formed by two valves corresponding to the carpel walls, is divided
57 longitudinally by the septum, which contains the transmitting tract and whose outer portion

58 becomes the replum. At the valve margins, between the replum and the valves, the dehiscence
59 zone is formed, herein two layers form, one is lignified and the adjacent one is unlignified.
60 The tension between the two during fruit maturation results in dehiscence and effective seed
61 dispersal (Ferrándiz, 2002; Ballester & Ferrándiz, 2017). Proper valve development is
62 ensured by the MADS-box transcription factor *FRUITFULL* (*FUL*), and replum identity is
63 the result of the maintained expression of the homeodomain *REPLUMLESS* (*RPL*) gene (Gu
64 *et al.*, 1998; Roeder *et al.*, 2003; Fourquin & Ferrándiz 2014). *FUL* and *RPL* act as repressors
65 of the MADS-box SHATTERPROOF proteins (SHP1 and SHP2) to the valve margin, which
66 in turn are responsible for the downstream activation of the bHLH genes, *INDEHISCENT*
67 (*IND*) in both the lignified and the separation layers, and of *ALCATRAZ* (*ALC*) and *SPATULA*
68 (*SPT*) only in the separation layer (Liljegren *et al.*, 2000; 2004; Rajani & Sundaresan 2001;
69 Girin *et al.*, 2011). Tension in these two layers during fruit maturation results in fruit
70 dehiscence at the valve margin, leaving the replum intact, and the seeds attached to it.

71 Homologs of these regulatory genes of fruit development have also been studied in
72 Solanaceae, in particular, in tomato and tobacco. Tomato has two functionally characterized
73 *FRUITFULL* orthologs, *SIFUL1* (named also *TDR4*) and *SIFUL2* (named also *MBP7*) that
74 are known to promote ripening during fruit development (Bemer *et al.*, 2012), and one
75 *SHATTERPROOF* homolog, *Tomato AGAMOUS-Like 1* (*TAGL1*). The *tagl1* mutant displays
76 ripening defects as well as reduction in the number of pericarp layers (Itkin *et al.*, 2009;
77 Vrebalov *et al.*, 2009; Pan *et al.*, 2010). *FUL* and *SHP* orthologs have also been functionally
78 characterized in tobacco dry dehiscent fruits of *Nicotiana* species. Over-expression of *NtFUL*
79 in *Nicotiana sylvestris* or down-regulation of *NbSHP* in *Nicotiana benthamiana* result in
80 indehiscent fruits, lacking a functional dehiscence zone (Fourquin & Ferrándiz 2012; Smykal
81 *et al.*, 2007). These data suggest that the *FUL-SHP* genetic switch is maintained in
82 Solanaceae (Fourquin & Ferrándiz 2012; Garceau *et al.* 2017). In addition to the structural
83 genes identified in *Arabidopsis*, other ripening genes have been identified in tomato,
84 including *SIMADS-RIN*, also a MADS-box transcription factor (Vrebalov *et al.* 2002; Ito *et*
85 *al.* 2017). Not only *SIMADS-RIN* controls softening along the maturation time course in
86 tomato (Fujisawa *et al.* 2011; 2012), but also the heterologous expression of the *Capsicum*
87 *annuum* ortholog *CaMADS-RIN* recovers the wild type phenotypes in *Slmads rin* mutant

88 backgrounds (Dong *et al.* 2013) suggesting that ripening via *RIN* occurs in both climacteric
89 tomato fruits and non-climacteric pepper fruits.

90 More recently we were able to study the downstream genes of *SHP* homologs in the
91 Solanaceae. The downstream targets comprise specifically the bHLH *ALCATRAZ/SPATULA*
92 genes, and orthologs of *INDEHISCENT/HECATE3*. These studies have shown that each gene
93 lineage has undergone different duplication time points resulting in different genetic
94 complements in the Solanaceae when compared to the Brassicaceae. In general, Solanaceae
95 species have less copies of *SHP* and lack *IND* orthologs. *IND* genes are the result of a
96 Brassicaceae specific duplication event, thus the Solanaceae have preduplication genes more
97 similar to *HEC3* than to *IND*. Both Solanaceae and Brassicaceae have the same number of
98 copies of *ALC* and *SPT* (Ortíz-Ramírez *et al.*, 2018). However, changes in copy number and
99 functional motifs within Solanaceae are hard to correlate to shifts in fruit type (dry/fleshy).
100 On the other hand, expression analyses done so far in four different Solanaceae species with
101 different fruit types show opposite expression of *SPT* and *ALC* orthologs between dry and
102 fleshy fruited species during fruit maturation. While *ALC* genes are turned off in the dry
103 dehiscent fruits of *Brunfelsia australis* during fruit maturation, *SPT* orthologs show this trend
104 of decreasing expression levels in fleshy fruits of *Capsicum annuum* and *Solanum*
105 *lycopersicum* during maturation (Ortíz-Ramírez *et al.*, 2018). Altogether, these data are
106 suggestive but insufficient to understand the functional contribution of the bHLH
107 downstream effectors in different Solanaceae fruit types.

108 Outside Brassicaceae and Solanaceae only a few other scattered expression studies of
109 *ALC/SPT bHLH* fruit development genes are available in strawberry (*Fragaria vesca*) and
110 peach (*Prunus persica*). In *P. persica*, expression analysis of the *SPT* ortholog,
111 *PPERALCATRAZ/SPATULA* (*PPERALC/SPT*), showed that it is expressed in the perianth,
112 ovary and later in the endocarp margins as well as in leaves (Tani *et al.* 2011; Dardick &
113 Callahan 2014). Based on these data, *PPERALC/SPT* was proposed to have a role in endocarp
114 patterning during fruit maturation. In *F. vesca* *FvSPT*, the *SPT* ortholog, is involved in
115 positively regulating fruit growth, as *faspt* fruits in early stages exhibited reduced size (Tisza
116 *et al.* 2010). The available data, however, are insufficient to assess if there are conserved
117 roles of *ALC/SPT* homologs in fruit development across different fruit types in different taxa.

118 In order to expand the functional analyses of *SPT* and *ALC* homologs, we have aimed to
119 assess spatio-temporal expression patterns and functions of *SPT* and *ALC* during vegetative
120 and reproductive development, and in particular their putative contribution to fruit
121 morphogenesis and development in different fruit types in Solanaceae. We have performed
122 *in situ* hybridization studies, as well as gene downregulation studies for *ALC* and *SPT*
123 homologs in one dry fruited species, *Nicotiana obtusifolia*, and in two fleshy fruited species,
124 *Capsicum annuum* cv Black Pearl and *Solanum lycopersicum* cv microTom. Our expression
125 analyses show overlapping and broad expression of *ALC* and *SPT* genes in the three species
126 during early flower development, but differences in their expression patterns according to
127 the fruit type at later stages. Our functional analyses show that *ALC* and *SPT* have roles in
128 floral organ growth, particularly petals, in the three species. In addition, both genes appear
129 to play redundant functions in limiting lignification and maintaining the identity of the
130 pericarp layers in both dry dehiscent and fleshy fruits. Finally, we found that *ALC/SPT* genes
131 participate in leaf pigmentation *via* the synthesis and accumulation of anthocyanins in
132 Solanaceae species, particularly those having dark green leaves. The roles in pigmentation
133 had been reported for other *bHLH* genes but not for those in the *ALC/SPT* gene lineage.

134

135 **Materials and Methods**

136 **Plant material and growth conditions**

137 *Capsicum annuum* cv. Black Pearl seeds were obtained from local supply stores, whereas
138 *Nicotiana obtusifolia* and *Solanum lycopersicum* var. microTom seeds were obtained from
139 the New York Botanical Garden (NYBG). All seeds were germinated on fertilized soil with
140 moisture control at 16h of light/ 8h of dark at 25°C. Seedlings were transplanted and grown
141 in the same conditions.

142 ***In situ* Hybridization**

143 For *in situ* hybridization, floral buds, carpels from anthetic flowers and fruits at different
144 developmental stages (F1 and F2) from wild type plants of *Nicotiana obtusifolia*, *Capsicum*
145 *annuum* and *Solanum lycopersicum* were collected and fixed under vacuum in freshly prepared
146 FAA (50% ethanol, 3.7% formaldehyde and 5% glacial acetic acid). Samples were
147 dehydrated, embedded and sectioned at 8-12µm on a Leica RM2125 rotary microtome. DNA

148 templates for RNA probe synthesis were obtained by PCR amplification of 400 to 550 bp
149 fragments. To ensure specificity, the primers were designed downstream of the bHLH region
150 that is highly variable between paralogs. RNA in situ hybridization was performed according
151 to Ferrándiz *et al.*, (2000) and optimized for each species: *N. obtusifolia* and *S. lycopersicum*
152 sections were hybridized overnight at 53°C, whereas *C. annuum* sections were hybridized
153 overnight at 55°C. For regular anatomy, material was fixed, embedded and sectioned as
154 described in Ortíz-Ramírez *et al.*, (2018).

155 **RNA extraction, PCR amplification and cloning of *ALCATRAZ* and *SPATULA* in the** 156 **TRV2-LIC vector**

157 Coding sequences of *ALC* and *SPT* genes were obtained from Sol Genomics Network
158 <https://solgenomics.net/> for all Solanaceae species available in the genera *Nicotiana*,
159 *Capsicum* and *Solanum* in public repositories, using the *Arabidopsis ALC* and *SPT* canonical
160 genes as queries. Isolated sequences have the following names: *NiobALC* and *NiobSPT* from
161 *Nicotiana obtusifolia* (GenBank numbers MK645609, MK645610), *CaanALC* and *CaanSPT*
162 from *Capsicum annuum* (GenBank numbers MK645607, MK645610), and *SlyALC*
163 (*Solyc04g078690.2.1*) and *SlySPT* (*Solyc02g093280.2.1*) from *Solanum lycopersicum*.

164 Total RNA extraction was performed from immature and mature fruits and leaves from three
165 different individuals of each species using TRizol reagent (Invitrogen). Total RNA was
166 DNaseI (Roche) treated to remove residual genomic DNA. Samples were quantified with
167 NanoDrop 2000 (Thermo Scientific). Three µg were used as template for cDNA synthesis
168 with SuperScript III reverse transcriptase (Invitrogen) using OligodT primers. The resulting
169 cDNA was used undiluted for amplification reactions by PCR using *ACTIN2* as a positive
170 control. *ALC* and *SPT* sequences were amplified with adaptor primers used in the LIC-VIGS
171 method following Dong *et al.* (2007). For each paralogous pair, the primers were designed
172 downstream of the bHLH region that is highly variable between *ALC* and *SPT* (Table S1).

173 The PCR products were purified with QuickPCR Purification Kit (PureLink, Invitrogen). A
174 total of 30ng of purified PCR product was treated with T4 DNA polymerase and 5mM dATP
175 at 22°C for 30 min followed by 20 min at 70°C for inactivation of T4 DNA polymerase. The
176 TRV2-LIC vector (pYY13; Dong *et al.*, 2007) was digested with PstI and similarly treated
177 with T4 DNA polymerase but dTTP replaced dATP. A total of 30ng of treated PCR product

178 and TRV2-LIC vector were mixed and incubated at 65°C for 2 min and then 22°C for 10 min
179 (Dong *et al.* 2007). Later 6µL of the mixture was transformed into *Escherichia coli* DHα5
180 competent cells by thermal shock and were grown in LB medium with 50µg/mL of
181 kanamycin. Positive clones were purified with Quick Plasmid Miniprep Kit (PureLink,
182 Invitrogen) and sequenced. Using this protocol, the following TRV2-LIC vectors were
183 generated: TRV2-*NiobALC*, TRV2- *NiobSPT*; TRV2-*CaanALC*, TRV2-*CaanSPT*; TRV2-
184 *SlyALC*, TRV2-*SlySPT* and TRV2-*NbPDS*. The latter included *Phytoene Desaturase* (PDS)
185 and was used as a positive control for transformation and target gene down-regulation (Liu
186 & Page., 2008).

187

188 **Agroinfiltration**

189 For the VIGS assay, TRV1 (pYL192; Liu *et al.* 2002) and TRV2-LIC (pYY13; Dong *et al.*
190 2007) vectors were introduced into the *Agrobacterium tumefaciens* strain GV3101 by
191 electroporation (BIO-RAD Gene Pulser Xcell), independently. A 5mL culture was grown
192 overnight at 28°C in selective medium with 50µg/mL of Kanamycin, 50µg/mL of
193 Gentamycin and 25µg/mL of Rifampicin. The next day, cultures were incubated in 500mL
194 of LB medium containing the same antibiotics, 1M MES, and 10mM acetosyringone. The
195 culture was grown 24h/28°C shaker. *Agrobacterium* cells were spun down and resuspended
196 in infiltration medium (autoclaved miliQ water with 10mM MES, 10mM MgCl₂, 200µM
197 acetosyringone), adjusted to an OD₆₀₀ of 2.0, and incubated at room temperature for 2 hours.
198 Combinations of TRV1, TRV2:*ALC* and TRV2:*SPT* were mixed in equal proportions 1:1:1
199 and inoculated with a syringe on the abaxial leaf surfaces of 50-65 seedlings per species. 20
200 seedlings per species were transformed with TRV1 and TRV2-LIC:*PDS*. In addition, 20
201 seedlings per species were transformed with TRV1 and TRV2:empty. 20 wild-type seedlings
202 per species were grown side by side with the transformed plants as a control. Infiltrated plants
203 were observed for 16 weeks and photographed with a digital camera CANNON RebelXT
204 200.

205 **Spectrophotometry**

206 Changes in leaf pigmentation exhibited by plants transformed with TRV2:*ALC* and
207 TRV2:*SPT* in *N. obtusifolia*, *C. annuum* and *S. lycopersicum* were further evaluated by

208 spectrophotometry. This is based on the physical phenomenon of selective absorption of
209 specific wavelengths by pigments, which are present in the plant leaves. Thus, changes in
210 pigmentation can be indirectly assessed by changes in the light absorption and reflection
211 (Van der Kooi *et al.*, 2016). Leaf squared pieces (approx. 5 x 5 mm) of three individuals per
212 species were used to measure the reflectance (i.e. the percentage of reflected/incident light)
213 in the visible range (350-800nm). A bifurcated optical probe (Avantes, Apeldoorn, The
214 Netherlands) was used connected to a spectrophotometer (Avaspec-2048, Avantes) with an
215 *AvaLight* light source composed of two lamps: deuterium (for UV radiation) and halogen
216 (visible range and close infrared). A white reference (WS-2, Avantes) was used as the
217 maximum reflectance control. All measurements were made in full darkness laboratory
218 space. The data were collected and stored with the *AvaSoft* program (Avantes). Finally, the
219 spectra were plotted with the Origin program.

220 **Scanning electron microscopy (SEM)**

221 For SEM studies, dehiscent fruits from both wild-type and VIGS downregulated plants of *N.*
222 *obtusifolia* were fixed in FAA and stored in 70% ethanol. Fruits were dehydrated through an
223 ethanol series and critical point dried using a Polaron E300. Material was mounted on
224 aluminum stubs with adhesive tabs (Electron Microscopy Sciences), sputter coated with gold
225 palladium and examined and photographed at 10 kV in a JEOL JSM-5410 scanning electron
226 microscope equipped with a CRIOSEM instrument CT 15000-C.

227 **Testing for Downregulation of *ALC* and *SPT* transcripts in the agroinfiltrated plants**

228 In order to test expression of *ALC* and *SPT* we selected young leaves of the wild type plants
229 as well as *ALC/SPT*-VIGS plants from the three species *N. obtusifolia*, *C. annuum*, and *S.*
230 *lycopersicum*. We performed total RNA extraction and cDNA synthesis as described above.
231 RT-PCR and qRT-PCR was used to evaluate *ALC* and *SPT* expression levels in putatively
232 downregulated plants in comparison to Wt and empty vector plants. Tissue selection and
233 collection in the plants was done following the color changes in the leaves detected in the
234 putatively downregulated plants (see results). Both light and dark regions of at least five
235 leaves per plant were collected. For qRT-PCR four out of the twenty plants (approx.)
236 screened by RT-PCR showing qualitative downregulation in agarose gels were further
237 selected. cDNAs was freshly made and diluted 1:4 as has been described in Pabón-Mora et

238 al., (2012). *UBIQUITIN-3* was selected from three additional endogenous controls tested
239 included *GAPDH*, β -*TUBULIN* and *Elongation Factor- 1 α* (*EF-1 α*) as it presented the lowest
240 variation in the Ct across samples. Target gene expression was evaluated in reference to
241 *UBIQUITIN-3* employing the $2^{-\Delta\Delta C_t}$ method for relative quantification (Livak & Schmittgen
242 2001). The data plotted includes standard deviations for three technical replicates. qRT-PCR
243 was done using the qPCR qTower3.0 system and the qPCRsoft software (Analytik Jena).
244 Independently cDNA from all RNA extractions was made using the TRV2 reverse primer in
245 order to screen for the presence of the viral vector in putatively downregulated plants. 3 μ g
246 of total RNA were used in the cDNA synthesis as described above. The PCR for TRV2 vector
247 screening was done with primers TRV2- Fwd and TRV2- Rev for 35 cycles at Tm 45°C. The
248 PCR product was run in agarose gels following the standard protocols.

249

250 **Results**

251 **Expression patterns of Solanaceae *ALCATRAZ/ SPATULA* genes**

252 We had previously found that all three species selected in this study, namely *Nicotiana*
253 *obtusifolia*, *Capsicum annuum* and *Solanum lycopersicum* have a single *ALCATRAZ* ortholog
254 and a single *SPATULA* ortholog (Ortiz-Ramírez *et al.*, 2018). To further investigate the
255 spatial and temporal expression patterns of *ALC* and *SPT* in Solanaceae, RNA *in situ*
256 hybridization was performed on floral buds at different developmental stages and in fruits
257 right after fertilization (i.e. F1 *sensu* Ortiz-Ramírez *et al.*, 2018) and at later stages of
258 development ranging between 3-4 days after fertilization of *N. obtusifolia*, *C. annuum* and *S.*
259 *lycopersicum*. The latter stage does not coincide with F2 *sensu* Ortiz-Ramírez *et al* (2018),
260 given that *in situ* hybridization at F2 was problematic due to secondary metabolite
261 accumulation in fleshy fruits and lignification in dry dehiscent fruits. *In situ* hybridization
262 with sense probes for all tested genes yielded no signal (Fig. S1).

263 The results show that both transcripts, *ALC* and *SPT*, have similar expression patterns in early
264 stages of flower development in the three species. *ALC* and *SPT* genes are expressed in all
265 floral organ primordia (Figs 1a-d, h-j; 2a-c, g-i; 3a-c, h-j). Expression during floral organ
266 development is present in sepals, petals, stamens and carpels in the three species, with some
267 species-specific differences (Figs 1a-d, h-j; 2a-c, g-i; 3a-c, h-j). In *N. obtusifolia*, *NiobALC*

268 (Fig. 1a-d) is more strongly expressed than *NiobSPT* (Fig. 1h-j), especially in sepal, petal and
269 stamen primordia. *NiobALC* and *NiobSPT* are also found at the distal most portion of the
270 petals and the carpel, as well as the placenta at later stages of flower development (Fig. 1c,
271 d, i, j). In *C. annuum* expression of both genes can be seen in all floral organ primordia (Fig.
272 2a-c, g-i) but as flower development progresses, *CaALC* and *CaSPT* transcripts concentrate
273 in the tips and the inner epidermis of the sepals and the petals (Figs 2c-f, i-k) as well as in
274 stamens and carpels (2d-f, 2j-l). In the gynoecium expression is detected in the carpel wall,
275 the stigma, the placenta and the ovules (Fig. 2e, f, k, l). In *S. lycopersicum*, *SlyALC* and
276 *SlySPT* are similarly expressed in sepal, petal, stamen and carpel primordia (Fig. 3a-e, h-l).
277 Both genes are maintained in preanthesis in the placenta where the nucellus will form, in the
278 developing ovules, and the distal most portion of the style and the stigma (Fig. 3b-e, k-l). In
279 addition, *SlySPT* expression is detected at the petal margins (Fig. 3j).

280 During fruit development, expression of *ALC* and *SPT* genes varies depending on the species.
281 In *N. obtusifolia*, with dry dehiscent fruits, *NiobALC* and *NiobSPT* genes are lowly expressed
282 in the pericarp and the developing seeds during day 1-2 after fertilization, that is, at early
283 stages of fruit and seed development (Fig. 1e, k). Both paralogs are first turned on during
284 fruit development in day 3 after fertilization, in what we will call hereafter “intermediate”
285 stages of fruit development, since this is after fertilization, but prior to endocarp lignification.
286 At this time point, *NiobALC* and *NiobSPT* are expressed in the endocarp, in an overlapping
287 region to where lignification will occur, and at the most distal portion of the fruit (Fig. 1f, g,
288 l, m). Thus, *NiobALC* and *NiobSPT* are more strongly expressed at the tip and the mid-level
289 of the fruit and are not detected at the base (Fig. 1f, l). In addition, both *NiobALC* and
290 *NiobSPT* are also turned on also in the developing seeds, specifically in the exotesta and the
291 developing embryo (Fig. 1f,g, l,m).

292 In *S. lycopersicum*, *SlyALC* and *SlySPT* have opposite expression patterns. *SlyALC* is turned
293 on early in fruit development at around days 1-3 after fertilization (Fig. 3f) and is maintained
294 afterwards between 6-9 days after fertilization, before cell expansion begins (Fig. 3g). In
295 particular, *SlyALC* transcripts are concentrated in the inner-most layers of the fruit wall (Fig.
296 3f, g). On the other hand, *SlySPT* is less expressed throughout the pericarp, and is only present
297 in early fruit developmental stages (Fig. 3m) and turned off at later stages (Fig. 3n).

298 Additionally, both genes are detected in the developing seeds closer to where the embryo
299 will develop (Fig. 3g, n).

300 **Functional analyses of Solanaceae *ALCATRAZ/SPATULA* genes**

301 In order to evaluate the function of *ALCATRAZ* and *SPATULA* genes in different species of
302 Solanaceae possessing different fruit types we used Virus Induced Gene Silencing (VIGS)
303 by employing the bipartite *Tobacco rattle virus* (TRV) to reduce of transcript levels of each
304 gene in the plant. At first, we generated single vectors for each gene and attempted to silence
305 each gene separately. However, there were no obvious phenotypes during flower or fruit
306 development in single downregulated plants where reduction in the level of *ALC* or *SPT* was
307 verified (Fig S2). Thus, we proceeded to downregulate simultaneously *ALC* and *SPT* in each
308 species.

309 Many of the plants simultaneously infiltrated with TRV2:*ALC* and TRV2:*SPT* had a first
310 obvious phenotype during vegetative growth related to a shift in coloration in the leaves (see
311 below). We began evaluating the transcript levels of *ALC* and *SPT* genes in the regions or
312 leaf patches showing lighter green areas in *ALC/SPT*-VIGS plants and to compare them with
313 Wt plants as well as empty-vector-treated plants, which never showed any changes in leaf
314 color (Fig. 4). In general, both the RT-PCR and the qRT-PCR showed a decrease in the
315 amount of endogenous transcripts of both *ALC* and *SPT* in the three species of 50-80% when
316 compared to Wt and empty vector treated plants. In addition, we were able to verify the
317 presence of TRV2 only in the *ALC/SPT*-VIGS plants confirming that TRV was active in
318 these downregulated lines (Fig. 4). Hereafter we will describe the phenotypes for each
319 species after simultaneous downregulation of *ALC* and *SPT*.

320 ***ALCATRAZ/SPATULA* genes control flower size and fruit development in *Nicotiana*** 321 ***obtusifolia***

322 A total of 65 plants were infiltrated with TRV1 and TRV2: *NiobALC* and TRV2: *NiobSPT*.
323 Hereafter these plants are referred to as *NiobALC/SPT*-VIGS. In 47% (n= 31) of the treated
324 plants, flowers displayed an overall reduction in size in pre-anthesis and anthesis, with shorter
325 sepals and less expanded petals (Fig. 5a-e). Petals were shorter in both the tubular portion
326 and the star-shaped frontal distal portion of the corolla (Fig. 5e). This reduction was more

327 obvious in the first flowers that developed after the treatment. Stamens and carpels were
328 likely also shorter as they still fitted in the smaller floral buds and flowers (Fig. 5c-e).

329 *NiobALC/SPT*-VIGS plants also showed changes in fruit development when compared to the
330 Wt plants, in particular, in terms of maturation timing and size. Wt fruits reached
331 approximately ~10.2 mm at ca. 14 days after fertilization, before dehiscence in our growth
332 conditions. Lignification occurred in the endocarp starting at 5DPA and it proceeded from
333 top to bottom of the fruit restricted to the two inner fruit wall layers of the endocarp (Fig. 5f-
334 h). *NiobALC/SPT*-VIGS fruits started maturing earlier, when the fruit was only ~5.3mm at
335 ca. 9 days after fertilization (Fig. 5i-j). Premature maturation leading to early fruit dehiscence
336 was accompanied by the typical basipetal lignification as well as the lignin deposition in an
337 additional fruit wall layer, resulting in three to four endocarp layers completely lignified as
338 opposed to the typical two to three such layers in Wt fruits (Fig. 5h, k).

339 Additional phenotypes were seen in the septum and placenta by SEM after ground tissue of
340 the placenta had dried and contracted, releasing the seeds. Wt fruits have an elongated and
341 winged septum with isodiametric and papillae like cells towards the middle region of the
342 placenta (Fig. 5l, m), while the *NiobALC/SPT*-VIGS fruits have an acute atypical apical
343 septum with flatter and unevenly spaced cells in the placenta (Fig. 5n, o).

344 ***ALCATRAZ/SPATULA* genes control petal fusion and fruit development in *Capsicum*** 345 ***annuum* and *Solanum lycopersicum***

346 For *C. annuum* a total of 60 plants were infiltrated with TRV1 and TRV2:*CaanALC* and
347 TRV2:*CaanSPT*; hereafter these plants are called *CaanALC/SPT*-VIGS. Similarly, 50 plants
348 of *S. lycopersicum* were infiltrated with TRV1 and TRV2:*SlyALC* and TRV2:*SlySPT*;
349 hereafter they are referred to as *SlyALC/SPT*-VIGS. Although the two species vary in terms
350 of the percentage of plants showing abnormal phenotypes when compared to the empty
351 vector and the Wt plants, in 87% (n= 52) of the *C. annuum* treated plants and in 73% (n= 37)
352 of the *S. lycopersicum* treated plants, the plants exhibit the phenotypes described below.

353 Wild type floral buds of *C. annuum* and *S. lycopersicum* exhibit protected floral buds with
354 complete postgenital petal fusion due to interlocking of trichomes at the margin of the petals,
355 that separate during anthesis (Fig. 6a-c; Fig. 7a-d). Both *CaanALC/SPT*-VIGS and
356 *SlyALC/SPT*-VIGS flowers display smaller petals as well as defects in petal fusion in young

357 floral buds resulting in premature exposure of developing stamens and carpels in preanthesis,
358 as well as petal asymmetry and unfused stamens during anthesis (Fig. 6d-f; Fig. 7e- h).

359 As it has been previously described, fleshy fruits of *C. annuum* and *S. lycopersicum*, are
360 characterized by having both periclinal and anticlinal cell division as well as cuticle
361 deposition (Pabón- Mora and Litt, 2011; Ortiz-Ramírez *et al.* 2018). The *C. annuum* fruits
362 exhibit also a clear differentiation of the two inner layers of the endocarp with respect to the
363 rest of the pericarp. The innermost layer of the endocarp is characterized by having small
364 parenchymatous cells and the one adjacent to it exhibits gigantic cells (almost 5-6 times the
365 normal cell size in the rest of the pericarp) with larger nuclei (Fig. 6g-i). The rest of the
366 endocarp, the mesocarp and the exocarp have parenchymatous cells with active cell division,
367 both anticlinal and periclinal (Fig. 6j). During maturation cell expansion in all layers occur
368 except in the inner endocarp whose cells undergo a change to sclerenchyma in parallel to the
369 expansion of the adjacent layer of gigantic cells. In addition, a cuticle develops over the
370 exocarp at late developmental stages (Fig. 6g-j). On the other hand, *S. lycopersicum* fruits
371 have a fully parenchymatous pericarp, also exhibiting anticlinal and periclinal cell division
372 in all fruit wall layers followed by cell expansion in the mesocarp and endocarp during fruit
373 growth and maturation. Unlike in *C. annuum* in *S. lycopersicum* the placenta protrudes and
374 surrounds the seeds. Most cells retain parenchymatous identity, with the exception of
375 collenchymatous cells in the mesocarp that provide the fruits with firmness to the touch
376 during maturation (Fig. i-l).

377 In addition to flower phenotypes, *CaanALC/SPT-VIGS* and *SlyALC/SPT-VIGS* plants
378 exhibit evident changes during fruit development when compared to wild type fruits.
379 *CaanALC/SPT-VIGS* and *SlyALC/SPT-VIGS* fruits reach similar sizes than those of the Wt
380 fruits but lack homogenous ripening, and exhibit striated pericarps with unripe areas (Fig.
381 6k-m; Fig. 7m-o). The *CaanALC/SPT-VIGS* fruits exhibited also embedded lignified
382 portions, in the form of sclerosomes (Fig. 6k-n). The *CaanALC/SPT-VIGS* fruits had
383 significant shifts in the firmness of the pericarp preserving the cuticle intact but with most of
384 the parenchymatic tissue in the mesocarp and endocarp entering lysogenic processes (Fig.
385 6k-n). Same ectopic lignification was seen in *SlyALC/SPT-VIGS* fruits occurring in parallel
386 to cell lysogeny in the parenchymatic areas of the endo and the mesocarp, however, lignified
387 areas occupied smaller areas when compared to the *C. annuum* fruits (Fig. 7o, p)

388

389 ***ALCATRAZ/SPATULA* genes have a role in leaf pigmentation**

390 Downregulation of *ALC* and *SPT* homologs in all three selected Solanaceae species resulted
391 in changes in leaf pigmentation. Double *ALC/SPT*-VIGS down-regulated plants exhibited
392 lighter green leaves (Fig. 8g, i, k), compared to wild type plants and control plants (TRV2:
393 empty) (Fig. 8a, c, e). All plants were grown under the same conditions; thus we believe that
394 changes are likely not occurring in response to nutritional deficiencies.

395 In order to quantitatively analyze the presence of specific pigments in wild type and down-
396 regulated *ALC/SPT*-VIGS plants, we performed spectrophotometric analyses from the Wt
397 and *ALC/SPT*-VIGS leaves from each species. In addition to this comparison, we used the
398 *Phytoene Desaturase (PDS)* down-regulated control plants. *PDS* encodes an enzyme in
399 carotenoid biosynthesis and silencing *pds* results in white leaf tissue due to photobleaching
400 (Fig. 8m, o, q). *PDS* downregulation is very efficient, is often 90% of the plants treated that
401 show photobleaching which is present in 7-10 leaves and often until flowering. For this
402 experiment, we compared the reflectance on the adaxial side of the Wt leaves with portions
403 of *ALC/SPT*-VIGS leaves that exhibited the light-green phenotype and to the *PDS*-VIGS
404 down-regulated plants having white leaves due to photobleaching.

405 The reflectance spectra show that the adaxial side of the wild type of *C. annuum* and *S.*
406 *lycopersicum* leaves are more similar to each other than to the *N. obtusifolia* (Fig. 8a-f). The
407 CaanWt and SlyWt leaves strongly absorb light between 400-510 nm and 570-700 nm, whilst
408 scattering in the green region (510-570 nm Fig. 8d, f). NiobWt leaves have similar absorption
409 ranges, reflecting in 510-650nm (Fig. 8b). This type of spectrum is typical of green leaves,
410 due to the presence of chlorophylls. Spectra of *ALC/SPT*-VIGS leaves in the three species
411 are more similar (Fig. 8g-l). These leaves absorb light between 400-500 nm and 650-700 nm
412 (Fig. 8h, j, l), just as the Wt type (Fig. 8b, d, f). However, a characteristic shoulder appears
413 in the reflectance between 550-650 nm with an increase of 5% when compared with Wt
414 leaves. This is presumably due to the reduction (or absence) of the pigments absorbing light
415 in this range.

416 As a comparison, the *PDS*-VIGS down-regulated leaves in the three species show continuous
417 reflectance throughout the visible and infrared part of the spectrum (400-800nm). This is an

418 expected feature of photobleached leaves (Fig. 8 m-r). All curves show absorption in the UV
419 range (below 400 nm) suggesting that absorption in this range is not affected by either
420 *ALC/SPT-VIGS* or *PDS-VIGS* downregulation. Fluctuations in the curves reveal the
421 presence of variable amounts of chlorophyll A and B due to incomplete silencing (Fig. 8h, j,
422 l).

423

424 **Discussion**

425 ***ALCATRAZ* and *SPATULA* function in positively controlling cell proliferation in floral** 426 **organs.**

427 Reduction in the *ALC* and *SPT* transcript levels in *N. obtusifolia*, *C. annuum* and *S.*
428 *lycopersicum* (Fig. 4) results in a reduction of flower and petal size, ectopic lignification in
429 the pericarp and shifts in leaf pigmentation (Fig. 5-8). *N. obtusifolia ALC/SPT-VIGS* plants
430 show a reduction in general floral size (Fig. 5) while *ALC/SPT-VIGS* plants in *S.*
431 *lycopersicum* and *C. annuum* downregulated plants exhibit particularly smaller petals
432 resulting in lack of postgenital petal fusion during floral growth and premature exposure of
433 stamens and carpels, as well as petal asymmetry during anthesis (Fig. 6; 7). These results
434 suggest that both *SolALC* and *SolSPT* have overlapping positive roles in cell proliferation
435 and/or expansion, in particular in the petal margins. Our observations show that these roles
436 coincide with the active and broad expression in tissues with high cell proliferation including
437 leaves and floral organs, and specifically petal margins and growing sepal tips in *N.*
438 *obtusifolia*, *C. annuum* and *S. lycopersicum* (Fig. 1-3; Ortiz-Ramírez *et al.*, 2018). Similar
439 expression of *ALC/SPT* homologs in young floral meristems, as well as all floral organs and
440 in particular sepal and petal tips has been observed in *Arabidopsis thaliana* (Heisler *et al.*
441 2001; Groszmann *et al.* 2010; 2011), *Prunus persica* (Tani *et al.* 2011) and *Bocconia*
442 *frutescens* (Zumajo- Cardona *et al.* 2017) suggesting that *ALC/SPT* likely control cell
443 proliferation in eudicots. However, they can promote or limit cell leaf and floral organ cell
444 proliferation, as in Brassicaceae they inhibit leaf and petal expansion (Penfield *et al.* 2005;
445 Ichihashi *et al.* 2010; Groszmann *et al.* 2010; 2011). while in Solanaceae they promote their
446 growth (Fig. 5-7).

447

448 Changes of the expression and function of orthologs in different plant families can occur due
449 to promoter regions responsive to upstream factors or to shifts in protein interaction partners.
450 Detailed studies of dissected promoter regions of *SPT* in *Arabidopsis* reveal that *SPT*
451 expression in proliferating meristems and young floral organs is mediated by the core
452 promoter region consisting of the E-box, TATA-box, and GA elements, which is bound by
453 *TCP* factors (Groszmann *et al.* 2010). This observation was linked to the role of *SPT* gene
454 function as activator of cell proliferation. In *Arabidopsis*, *ALC* and *SPT* are also expressed in
455 mature tissues like the petals, the endocarp, the nectaries, the hypocotyl, the stem and the leaf
456 stomata (Heisler *et al.* 2001; Groszmann *et al.* 2010; 2011). Groszmann *et al.* (2010),
457 identified general enhancers as well as tissue specific enhancers and silencers by targeted
458 promoter deletions for *SPT* and highlighted the importance of binding sites for the *bona fide*
459 cell proliferation *TCP* transcription factors. Less information is available for *ALC*, as no
460 promoter studies have been done in this gene in *Arabidopsis*, however, it has been shown
461 that *ALC* and *SPT* share regulatory regions like the E-box, elements involved in valve margin
462 activation and the dehiscence zone as well as GA responsive elements (Groszmann *et al.*
463 2010; 2011). These shared elements could help explain the overlapping expression of both
464 paralogs, not only in Brassicaceae (Groszmann *et al.* 2010; 2011), but also in Solanaceae
465 (Figs. 1-3). A possible change in function of *ALC/SPT* genes between the two plant families
466 due to the presence of *TCP* responsive elements and the specificity of such activation will
467 require promoter mutation studies in Solanaceae species. In addition to changes in response
468 to specific *TCP* genes, shifts between the roles of *ALC/SPT* genes in growing leaves and
469 floral organs could be linked to protein partner specificity in protein-protein interactions,
470 controlling different processes. This is supported by the extensive changes documented in
471 the coding sequences of *ALC* and *SPT* orthologs between Brassicaceae and Solanaceae,
472 pointing to massive reduction of *ALC* in *Arabidopsis* relatives when compared to most
473 Solanaceae species and the loss of several protein motifs (Pabón-Mora *et al.*, 2014; Ortíz-
474 Ramírez *et al.*, 2018). Functional characterization of specific motifs in Solanaceae sequences
475 will have to be addressed in order to identify which are more important for their function in
476 promoting leaf and petal growth.

477

478 **The role of Solanaceae *ALCATRAZ/ SPATULA* genes in gynoecium development and**
479 **fruit histogenesis.**

480 In *Arabidopsis* *ALC* and *SPT* possess partially redundant functions during gynoecium
481 development, as double mutants exhibit delayed medial growth and enhanced fusion defects
482 when compared to the single mutants (Groszmann *et al.* 2011). In the Solanaceae species
483 here studied, both genes have overlapping expression in the gynoecium and particularly in
484 the style and stigma (Fig. 1-3), similarly to the paralogs in *P. persica* (Tani *et al.*, 2011) and
485 *B. frutescens* (Zumajo- Cardona *et al.* 2017) suggesting that in fact they could redundantly
486 control gynoecium medial growth and distal fusion, like in *Arabidopsis*. Previous
487 complementation studies overexpressing *Solanum lycopersicum* *LsSPT* rescue the *spt2*
488 mutant in *Arabidopsis* and show full restoration of gynoecium apical fusion and silique
489 length, suggesting that *SPT* orthologs play similar roles in distantly related species
490 (Groszmann *et al.*, 2008). However, our downregulated *ALC/SPT*-VIGS plants for all three
491 species *N. obtusifolia*, *C. annuum*, and *S. lycopersicum* do not exhibit phenotypic differences
492 with respect to the wild type plants in the gynoecium. These results suggest that either (1)
493 downregulation levels allow for residual activity of *ALC/SPT* genes in VIGS plants, or (2)
494 other transcription factors acting independently from *ALC/SPT* genes in this function
495 compensate for the reduced transcript levels in the downregulated plants. Additional
496 candidate genes that may be playing redundant roles in distal gynoecium patterning are *STY*
497 or *NGA*, both involved in style and stigma development (Gomariz-Fernández *et al.* 2017).

498 As for fruit development, previous studies have shown that *FUL*, *SHP*, *IND* and *ALC*
499 orchestrate a transcription factor network that controls the formation of the dehiscence zone
500 and tissue differentiation in the valve margins of the *Arabidopsis* silique (Liljegren *et al.*
501 2004). *FUL* negatively regulates *SHP1/2* expression (Ferrández *et al.* 2000), while the latter
502 activates the expression of *IND* and *ALC* in the valve margins, where the two genes are
503 involved in determining the lignified layer and the separation layer, respectively (Liljegren
504 *et al.* 2000; 2004). In this network *ALC* plays a decisive role during fruit histogenesis as
505 demonstrated by the *alc* mutant where the separation layer (adjacent to the lignified layer) is
506 not properly formed resulting in ectopic lignification in the form of a “bridging zone”
507 connecting the valve margin with the replum, and resulting in indehiscent fruits (Rajani &
508 Sundaresan 2001). Thus, *ALC* is likely playing a direct or indirect role in preventing

509 lignification to occur in the separation layer during fruit patterning (Rajani & Sundaresan
510 2001; Roeder & Yanofsky 2006). Additional functional studies have defined *ALC* and *SPT*
511 as partially redundant, likely linked to incipient subfunctionalization where *SPT* plays
512 prevalent roles during gynoecium development and *ALC* is more important during fruit
513 histogenesis and development (Groszmann *et al.* 2011). Similar trends to
514 subfunctionalization, or at least function redistribution among paralogs is also seen in *Prunus*
515 *persica*. In this rosid, the first tier of genetic regulation, the *FUL-SHP* antagonistic relationship
516 is likely maintained, as *PPERFUL* is predominantly expressed in the meso and exocarp, non-
517 overlapping with *PPERSHP* restricted to the endocarp (Tani *et al.* 2007; Dardick *et al.* 2010;
518 Fourquin & Ferrándiz 2014). The second tier in the genetic cascade involving *ALC* and *SPT*
519 shows also a trend to subfunctionalization as the *ALC* ortholog is restricted to the exo and
520 mesocarp, while the *SPT* ortholog is restricted to the endocarp. Because their expression is
521 non overlapping in this particular fruit type (the drupe) it has been suggested that *ALC* and
522 *SPT* are likely specializing in specifying different cell layers during fruit development (Tani
523 *et al.* 2007; 2011; Dardick *et al.* 2010).

524 There are three aspects that are important to consider up to this point: (1) *ALC* orthologs are
525 expressed throughout fruit development in fleshy fruits of *C. annuum* and *S. lycopersicum*
526 while they are only expressed prior to endocarp lignification in intermediate developmental
527 fruit stages in dry dehiscent fruits of *N. obtusifolia* (Fig. 1-3; Ortiz- Ramírez *et al.*, 2018). (2)
528 *SPT* orthologs have a different expression pattern, as they are turned off during berries
529 maturation but they are turned on in intermediate to late stages of fruit development in the
530 endocarp of dry dehiscent fruits of *N. obtusifolia* (Fig. 1-3; Ortiz- Ramírez *et al.*, 2018);
531 finally, (3) Downregulated *ALC/SPT*-VIGS plants for both genes in the three species here
532 studied exhibit ectopic (and/or early) lignification in the pericarp independently of the fruit
533 type (Fig. 5-7). Considering these aspects, we suggest that in dry dehiscent fruits of *Nicotiana*
534 *obtusifolia*, *NiobALC* and *NiobSPT* are likely involved in delimiting cell differentiation in
535 the endocarp, as their expression patterns are localized only to these cell layers prior to
536 lignification. However, as *Niob ALC/SPT*-VIGS plants exhibit premature and ectopic
537 lignification, we believe *NiobALC* and *NiobSPT* can be negatively regulate premature
538 lignification in the endocarp in wild type fruits during fruit maturation (Fig. 5). Conversely,
539 in fleshy fruits of *C. annuum* and *S. lycopersicum*, the *ALC* orthologs possibly play a more

540 important role than *SPT* orthologs in fruit patterning and maturation. We believe so, because
541 *ALC* homologs are expressed during early and late fruit development in higher amounts than
542 *SPT* homologs, and because *SPT* is turned off during maturation (Figs. 2, 3). Nevertheless,
543 both genes *ALC* and *SPT* are likely repressing lignification in a redundant manner, in favor
544 of maintaining parenchymatous tissue in the pericarp, continuously like in fleshy fruits or
545 momentarily in dry dehiscent fruits. This is supported by the observation that downregulated
546 fleshy fruits for both genes form striate fruits with patched pericarps presenting
547 sclerenchymatic zones (Fig. 6, 7). Thus, *SPT* and *ALC* genes in Solanaceae are likely to
548 have a role in repressing lignification in both time and space during fruit patterning and
549 maturation, similar to their role in *Arabidopsis*, where they provide the identity of the
550 separation layer in the dehiscence zone (Rajani & Sundaresan 2001). Here, it is important to
551 highlight, that these conclusions are based on VIGS double silenced lines, as single gene
552 downregulated plants did not show fruit abnormal phenotypes compared to the wild type
553 plants. With genome editing techniques, it may be possible to unravel the contribution of
554 each gene independently in a more precise manner. Additionally, more detailed functional
555 analyses will have to be done in other plant families with different fruit types outside
556 Solanaceae to test the putative role of *ALC* and *SPT* during fruit histogenesis, and to better
557 understand how these genes may be controlled in time and space to form dry dehiscent and
558 fleshy fruits.

559

560 **The co-option of *ALCATRAZ/SPATULA* genes in leaf pigmentation.**

561 The double *ALC/SPT*-VIGS plants in the three species *N. obtusifolia*, *C. annuum*, and *S.*
562 *lycopersicum* exhibit defects in leaf pigmentation. This is evident by the shift in light
563 reflectance between 550-650nm (Fig. 8) suggesting that they are linked to the production or
564 accumulation of pigments that are involved in photo-protection, in particular given the
565 wavelength change of anthocianins. This is also indicated by the more obvious leaf lightening
566 occurring in the darker leaves of *C. annuum* than in those already slightly light green in *S.*
567 *lycopersicum* and *N. obtusifolia*. Anthocianins are a type of flavonoids that are synthesized
568 using the phenylpropanoid pathway, where the substrate p-coumaroyl CoA is common
569 between the flavonoid as well as the lignin biosynthesis (Besseau *et al.* 2007). Anthocyanins

570 have a broad absorption range at the end of the blue light in the visible spectrum between
571 520-540 nm, thus, this range is often used in spectrophotometer measurements to indicate
572 anthocyanin accumulation (Horbowicz *et al.* 2008; Akond *et al.* 2011). Importantly
573 anthocyanins as well as UV absorbing flavonoid pigments in flowers are more frequently
574 located solely in the epidermal layers, contrary to other pigments like carotenoids that occur
575 and accumulate in the epidermises and the mesophyll (Kay *et al.*, 1981). However, in leaves
576 they can accumulate more broadly in the mesophyll, where it is possible that they act as
577 scavengers of oxygen radicals produced by chloroplasts (Strack *et al.*, 1982; Schulz &
578 Weissenböck, 1986; Gould *et al.* 2000). Traditionally invasive techniques like high
579 performance liquid chromatography (HPLC) and mass spectrometry (MS), are necessary to
580 identify chemical compounds present in vegetative tissues. However, recent research in
581 different colored petals has shown that color can be dissected out and measured as the
582 combined effect of pigment absorption spectrum, scattering structures and petal thickness
583 (Van der Kooi *et al.* 2016). Like these authors we have implemented spectrophotometer
584 measurements in fresh leaves from *ALC/SPT*-VIGS down regulated plants in order to test for
585 changes in specific pigments, in this case the anthocyanins.

586 Our results, revealing a loss in pigments absorbing between 520-550nm, show that it is likely
587 that *ALC* and *SPT* genes have become integrated into leaf flavonoid biosynthesis in
588 Solanaceae species. This may occur in a similar manner to that shown for other bHLH genes
589 like *GLABRA3 (GL3)*, *ENHANCER OF GLABRA3 (EGL3)* and *TRANSPARENT TESTA8*
590 (*TT8*) that have been linked to the biosynthesis and accumulation of anthocyanins in
591 vegetative tissues in *Arabidopsis* (Feller *et al.* 2011; Xu *et al.* 2015). In the latter case, the
592 bHLH genes are part of larger regulatory complexes known as MBW, where there is one
593 MYB gene component interacting directly with a bHLH gene and the two of them physically
594 interacting with a third gene WD40, hence the name MBW (Nesi *et al.*, 2000; Baudry *et al.*,
595 2004; Xu *et al.* 2015). The same complexes with other genes belonging to the same gene
596 families are known to regulate trichome development, radicular hairs and mucilage synthesis
597 covering the seeds (Besseau *et al.* 2007; Xu *et al.* 2015). Our comparative alignments for
598 bHLH genes in Solanaceae species revealed little similarity between the *ALC /SPT* genes,
599 belonging to subgroup VII (a+b) *sensu* Pires & Dolan (2010) and the bHLH genes typically
600 linked to anthocyanin synthesis mentioned above, belonging to clade IIIIF (Pires & Dolan

601 2010; Feller *et al.* 2011; Fig. S3; Table S2). The same comparisons overruled a possible off-
602 target silencing effect, as the regions included in the TRV2 vector for downregulation flank
603 the region downstream the bHLH domain where the genes from the two subgroups are highly
604 divergent (Atchley *et al.*, 1999). Altogether, our data points to a likely co-option of *ALC/SPT*
605 genes in the biosynthesis of anthocyanins in the leaves of Solanaceae species. However, it is
606 unclear what are the specific molecular mechanisms employed in this cascade and we can
607 only speculate that MBW complexes are flexible enough to integrate other bHLH partners
608 besides the classical *GL3*, *EFGL3* and *TT8* in pigment accumulation and synthesis in other
609 species outside *Arabidopsis*.

610

611 **Acknowledgements**

612 This work was funded by COLCIENCIAS (111565842812), the iCOOP + 2016
613 COOPB20250 from the Centro Superior de Investigación Científica, CSIC, the ExpoSeed
614 (H2020.MSCA-RISE-2015-691109) EU grant, the Convocatoria Programáticas 2017-16302,
615 and the Estrategia de Sostenibilidad 2018-2019, from the Universidad de Antioquia. We
616 would like to thank the group members of the Ferrándiz and Madueño labs at IBMCP- UPV
617 for training and help in the standardization of *in situ* hybridization. Finally, we thank Ricardo
618 Callejas and Zulma Monsalve, from the Universidad de Antioquia for their helpful
619 suggestions during this research.

620

621 **Author Contributions**

622 C.I.O-R, C.F, and N.P-M planned and designed the research. All authors performed
623 experiments, analyzed the data and wrote and approved the final version of the manuscript.

624 **ORCID**

625 Natalia Pabón-Mora ORCID: 0000-0003-3528-8078

626 **Supporting information**

627 **Fig. S1** Sense probes of all genes resulted in no signal in the *In situ* hybridization analyses.

628 **Fig. S2.** Phenotypes recorded for the singly downregulated *NiobSPT*, *NiobALC*, *CaanSPT*
629 and *CaanALC* VIGS plants.

630 **Fig. S3** Alignments for ALCATRAZ and SPATULA protein with the bHLH genes typically
631 linked to anthocyanin synthesis of Solanaceae and *Arabidopsis*.

632 **Table S1** Primers used for all the experiments.

633 **Table S2** Accession numbers for all sequences used in alignments for ALCATRAZ and
634 SPATULA protein with the bHLH genes typically linked to anthocyanin synthesis of
635 Solanaceae and *Arabidopsis*.

636

637 **References**

638 **Akond ASM, Khandaker L, Bethold J, Gates L, Peters K, Delong H, Hossain K. 2011.**
639 Anthocyanin, total polyphenols and antioxidant activity of common bean. *American Journal*
640 *of Food Technology* **6**: 385–394.

641 **Atchley WR, Therhalle W, Dress A. 1999.** Positional dependence, cliques and predictive
642 motifs in the bHLH protein domain. *Journal of Molecular Evolution* **48**: 501–516.

643 **Ballester P, Ferrándiz C. 2017.** Shattering fruits: variations on a dehiscent theme. *Current*
644 *Opinion in Plant Biology* **35**: 68-75.

645 **Baudry A, Heim MA, Dubreucq B, Caboche M, Weisshaar B, Lepiniec L. 2004.** TT2,
646 TT8, and TTG1 synergistically specify the expression of *BANYULS* and proanthocyanidin
647 biosynthesis in *Arabidopsis thaliana*. *The Plant Journal* **39**: 366–380.

648 **Bemer M, Karlova R, Ballester AR, Tikunov YM, Bovy AG, Wolters-Arts M, Rossetto**
649 **PB, Angenent GC, de Maagd R. 2012.** The Tomato *FRUITFULL* Homologs TDR4/FUL1
650 and MBP7/FUL2 Regulate Ethylene-Independent Aspects of Fruit Ripening. *The Plant Cell*
651 **24**: 4437–4451.

652 **Besseau S, Hoffman L, Geoffroy P, Lapierre C, Pollet B, Legrand M. 2007.** Flavonoid
653 Accumulation in *Arabidopsis* Repressed in Lignin Synthesis Affects Auxin Transport and
654 Plant Growth. *The Plant Cell* **19**: 148–162.

655 **Dardick CD, Callahan AM. 2014.** Evolution of the fruit endocarp: molecular mechanisms
656 underlying adaptations in seed protection and dispersal strategies. *Frontiers in Plant Science*
657 **5**: 1–10.

658 **Dardick CD, Callahan AM, Chiozzotto R, Schaffer RJ, Piagnani MC, Scorza R. 2010.**
659 Stone formation in peach fruit exhibits spatial coordination of the lignin and flavonoid
660 pathways and similarity to *Arabidopsis* dehiscence. *BMC Biology* **8**: 1–17.

661 **Dinneny JR, Weigel D, Yanofsky MF. 2005.** A genetic framework for fruit patterning in
662 *Arabidopsis thaliana*. *Development* **132**: 4687-4696.

663 **Dong T, Hu Z, Deng L, Wang Y, Zhu M, Zhang J, Chen G. 2013.** A Tomato MADS-Box
664 Transcription Factor, SIMADS1, Acts as a Negative Regulator of Fruit Ripening. *Plant*
665 *Physiology* **163**: 1026–1036.

666 **Dong Y, Burch-Smith TM, Liu Y, Mamillapalli P, Dinesh-Kumar SP. 2007.** A Ligation-
667 Independent Cloning Tobacco Rattle Virus Vector for High-Throughput Virus-Induced Gene
668 Silencing Identifies Roles for NbMADS4-1 and -2 in Floral Development. *Plant Physiology*
669 **145**: 1161–1170.

670 **Esau K. 1967.** *Plant Anatomy*, 2nd Ed. New York: John Wiley.

671 **Feller A, MacHemer K, Braun EL, Grotewold E. 2011.** Evolutionary and comparative
672 analysis of MYB and bHLH plant transcription factors. *The Plant Journal* **66**: 94–116.

673 **Ferrándiz C. 2002.** Regulation of fruit dehiscence in *Arabidopsis*. *Journal of Experimental*
674 *Botany* **53**: 2031–2038.

675 **Ferrándiz C, Liljegren SJ, Yanofsky MF. 2000.** Negative regulation of the
676 SHATTERPROOF genes by FRUITFULL during *Arabidopsis* fruit development. *Science*
677 **289**: 436–438.

678 **Fourquin C, Ferrándiz C. 2012.** Functional analyses of *AGAMOUS* family members in
679 *Nicotiana benthamiana* clarify the evolution of early and late roles of C-function genes in
680 eudicots. *The Plant Journal* **71**: 990–1001.

681 **Fourquin C, Ferrándiz C. 2014.** The essential role of *NGATHA* genes in style and stigma
682 specification is widely conserved across eudicots. *New Phytologist* **202**: 1001–1013.

683 **Fujisawa M, Nakano T, Ito Y. 2011.** Identification of potential target genes for the tomato
684 fruit-ripening regulator RIN by chromatin immunoprecipitation. *BMC Plant Biology* **11**:26.

685 **Fujisawa M, Shima Y, Higuchi N, Nakano T, Koyama Y, Kasumi T, Ito Y. 2012.** Direct
686 targets of the tomato-ripening regulator RIN identified by transcriptome and chromatin
687 immunoprecipitation analyses. *Planta* **235**: 1107–1122.

688 **Garceau DC, Batson MK, Pan IL. 2017.** Variations on a theme in fruit development: the
689 PLE lineage of MADS-box genes in tomato (*TAGL1*) and other species. *Planta* **246**: 313–
690 321.

691 **Girin T, Paicu T, Stephenson P, Fuentes S, Körner E, O'Brien M, Sorefan K, Wood**
692 **TA, Balanzá V, Ferrándiz C, Smyth D, Østergaard L. 2011.** INDEHISCENT and
693 SPATULA Interact to Specify Carpel and Valve Margin Tissue and Thus Promote Seed
694 Dispersal in *Arabidopsis*. *Plant Cell* **23**: 3641–3653.

695 **Gomariz-Fernández A, Sánchez-Gerschon V, Fourquin C, Ferrándiz C. 2017.** The Role
696 of SHI/STY/SRS Genes in Organ Growth and Carpel Development Is Conserved in the

697 Distant Eudicot Species *Arabidopsis thaliana* and *Nicotiana benthamiana*. *Frontiers in Plant*
698 *Science* **8**: 814.

699 **Gould KS, Markham KR, Smith RH, Goris JJ. 2000.** Functional role of anthocyanins in
700 the leaves of *Quintinia serrata* A. Cunn. *Journal of Experimental Botany* **51**: 1107–1115.

701 **Groszmann M, Paicu T, Smyth D. 2008.** Functional domains of SPATULA, a bHLH
702 transcription factor involved in carpel and fruit development in *Arabidopsis*. *The Plant*
703 *Journal* **55**: 40-52.

704 **Groszmann M, Bylstra Y, Lampugnani ER, Smyth DR. 2010.** Regulation of tissue-
705 specific expression of SPATULA, a bHLH gene involved in carpel development, seedling
706 germination, and lateral organ growth in *Arabidopsis*. *Journal of Experimental Botany* **61**:
707 1495–1508.

708 **Groszmann M, Paicu T, Alvarez JP, Swain SM, Smyth DR. 2011.** SPATULA and
709 ALCATRAZ, are partially redundant, functionally diverging bHLH genes required for
710 *Arabidopsis* gynoecium and fruit development. *Plant Journal* **68**: 816–829.

711 **Gu Q, Ferrándiz C, Yanofsky MF, Martienssen R. 1998.** The FRUITFULL MADS-box
712 gene mediates cell differentiation during *Arabidopsis* fruit development. *Development* **125**:
713 1509–1517.

714 **Heisler MG, Atkinson A, Bylstra YH, Walsh R, Smyth DR. 2001.** SPATULA, a gene that
715 controls development of carpel margin tissues in *Arabidopsis*, encodes a bHLH protein.
716 *Development* **128**: 1089–1098.

717 **Horbowicz M, Kosson R, Grzesiuk A, Dębski H. 2008.** Anthocyanins of Fruits and
718 Vegetables - Their Occurrence, Analysis and Role in Human. *Vegetable Crops Research*
719 *Bulletin* **68**: 5–22.

720 **Ichihashi Y, Horiguchi G, Gleissberg S, Tsukaya, H. 2010.** The bHLH transcription factor
721 SPATULA controls final leaf size in *Arabidopsis thaliana*. *Plant Cell Physiology* **51**: 252–
722 261.

723 **Itkin M, Seybold H, Breitel D, Rogachev I, Meir S, Aharoni A. 2009.** TOMATO
724 AGAMOUS-LIKE 1 is a component of the fruit ripening regulatory network. *Plant Journal*
725 **60**: 1081–1095.

726 **Ito Y, Nishizawa-Yokoi A, Endo M, et al. 2017.** Re-evaluation of the rin mutation and the
727 role of RIN in the induction of tomato ripening. *Nature Plants* **3**: 866–874.

728 **Kay QON, Daoud HS, Stirton CH. 1981.** Pigment distribution, light reflection and cell
729 structure in petals. *Botanical Journal of the Linnean Society* **83**: 57–83.

730 **Liljegren SJ, Roeder AH, Kempin SA, Gremski K, Østregård L, Guimil S, Reyes DK,**
731 **Yanofsky MF. 2004.** Control of fruit patterning in *Arabidopsis* by INDEHISCENT. *Cell*
732 **116**: 843–853.

733 **Liljegren SJ, Ditta GS, Esched Y, Savidge B, Bowman JL, Yanofsky MF. 2000.**
734 SHATTERPROOF MADS-box genes control seed dispersal in *Arabidopsis*. *Nature* **404**:
735 766–770.

736 **Liu Y, Schiff M, Marathe R, Dinesh-Kumar SP. 2002.** Tobacco Rar1, EDS1 and
737 NPR1/NIM1 like genes are required for N-mediated resistance to tobacco mosaic virus. *Plant*
738 *Journal* **30**: 415–429.

739 **Liu E, Page JE. 2008.** Optimized cDNA libraries for virus-induced gene silencing (VIGS)
740 using tobacco rattle virus. *Plant Methods* **4**: 5.

741 **Livak KJ, Schmittgen TD. 2001.** Analysis of relative gene expression data using real-time
742 quantitative PCR and the $2^{-\Delta\Delta CT}$ method. *Methods* **25**: 402–408.

743 **Nesi N, Debeaujon I, Jond C, Pelletier G, Caboche M, Lepiniec L. 2000.** The *TT8* gene
744 encodes a basic helix-loop-helix domain protein required for expression of *DFR* and *BAN*
745 genes in *Arabidopsis* siliques. *The Plant Cell* **12**: 1863–1878.

746 **Ortíz-Ramírez CI, Plata-Arboleda S, Pabón-Mora N. 2018.** Evolution of genes associated
747 with gynoecium patterning and fruit development in Solanaceae. *Annals of Botany* **121**:
748 1211-1230.

749 **Pabón-Mora N, Ambrose B, Litt A. 2012.** Poppy APETALA1/FRUITFULL orthologs
750 control flowering time, branching, perianth identity, and fruit development. *Plant Physiology*
751 **158**: 1685-1704.

752 **Pabón-Mora N, Wong KG, Ambrose B. 2014.** Evolution of fruit development genes in
753 flowering plants. *Frontiers of Plant Science* **5**: 300.

754 **Pan IL, McQuinn R, Giovannoni JJ, Irish VF. 2010.** Functional diversification of
755 AGAMOUS lineage genes in regulating tomato flower and fruit development. *Journal of*
756 *Experimental Botany* **61**: 1795–1806.

757 **Penfield S, Josse EM, Kannangara R, Gilday AD, Haliday KJ, Graham IA. 2005.** Cold
758 and light control seed germination through the bHLH transcription factor SPATULA.
759 *Current Biology* **15**: 1998–2006.

760 **Pires N, Dolan L. 2010.** Origin and diversification of basic-helix-loop-helix proteins in
761 plants. *Molecular Biology and Evolution* **27**: 862–874.

762 **Rajani S, Sundaesan V. 2001.** The *Arabidopsis* myc/bHLH gene *ALCATRAZ* enables cell
763 separation in fruit dehiscence. *Current Biology* **11**: 1914–1922.

764 **Roeder AHK, Yanofsky MF. 2006.** Fruit Development in *Arabidopsis*. The *Arabidopsis*
765 Book.

766 **Roeder AHK, Ferrándiz C, Yanofsky MF. 2003.** The role of the REPLUMLESS
767 homeodomain protein in patterning the *Arabidopsis* fruit. *Current Biology* **13**: 1630–1635.

768 **Schulz M, Weissenböck G. 1986.** Isolate and separation of epidermal and mesophyll
769 protoplast from rye primary leaves- tissue- specific characteristics of secondary phenolic
770 product accumulation. *Zeitschrift für Naturforschung* **41c**: 22-27.

771 **Seymour GB, Østergaard L, Chapman NH, Knapp S, Martin C. 2013.** Fruit
772 Development and Ripening. *Annual Review in Plant Biology* **64**: 219–241.

773 **Smykal P, Gennen J, De Bodt S, Ranganath V, Melzer S. 2007.** Flowering of strict
774 photoperiodic Nicotiana varieties in non-inductive conditions by transgenic approaches.
775 *Plant Molecular Biology* **65 (3)**: 233-242.

776 **Strack D, Meurer B, Weissenböck G. 1982.** Tissue- specific kinetics of flavonoid
777 accumulation in primary leaves of rye (*Secale cereale L.*). *Zeitschrift für Naturforschung.*
778 **108**:131-141.

779 **Tani E, Tsballa A, Stedel C, Kallonati C, Papaethimiou D, Polidoros A, Darzentas N,**
780 **Ganopoulos I, Fletmetakis E, Katinakis P, Tsaftaris A. 2011.**The study of a SPATULA-
781 like bHLH transcription factor expressed during peach (*Prunus persica*) fruit development.
782 *Plant Physiology and Biochemistry* **49**: 654–663.

783 **Tani E, Polidoros AN, Tsaftaris AS. 2007.**Characterization and expression analysis of
784 FRUITFULL- and SHATTERPROOF-like genes from peach (*Prunus persica*) and their role
785 in split-pit formation. *Tree Physiology* **27**: 649–659.

786 **Tisza V, Kovács L, Balogh A, Heszky L, Kiss E. 2010.** Characterization of FaSPT, a
787 SPATULA gene encoding a bHLH transcriptional factor from the non-climacteric strawberry
788 fruit. *Plant Physiology and Biochemistry* **48**: 822–826.

789 **Van der Kooi CJ, Elzenga JTM, Staal M, Stavenga DG. 2016.** How to colour a flower:
790 on the optical principles of flower coloration. *Proceedings of the Royal Society B* **283**:
791 20160429.

792 **Vrebalov J, Ruezinsky D, Padmanabhan V, White R, Medrano D, Drake R, Schuch W,**
793 **Giovannoni J, 2002.** A MADS-box gene necessary for fruit ripening at the tomato ripening-
794 inhibitor (*rin*) locus. *Science* **296**: 343–346.

795 **Vrebalov J, Pan IL, Matas-Arroyo J, McQuinn R, Chung MY, Poole M, Rose J,**
796 **Seymour G, Grandillo S, Giovannoni J, Irish VF. 2009.** Fleshy Fruit Expansion and
797 Ripening Are Regulated by the Tomato SHATTERPROOF Gene TAGL1. *The Plant Cell*
798 **21**: 3041–3062.

799 **Xu W, Dubos C, Lepiniec L. 2015.** Transcriptional control of flavonoid biosynthesis by
800 MYB-bHLH-WDR complexes. *Trends in Plant Science* **20**: 176–185.

801 **Zumajo-Cardona C, Ambrose BA, Pabón-Mora N. 2017.** Evolution of the
802 SPATULA/ALCATRAZ gene lineage and expression analyses in the basal eudicot,
803 *Bocconia frutescens L.* (*Papaveraceae*). *Evo Devo* **8**: 1–18.

804

805 **Figure legends**

806 **Fig. 1** Expression analyses by *In situ* Hybridization of *NiobALC* (a-g) and *NiobSPT* (h-m) in
807 floral buds (a-d, h-j) and fruits (e-g, k-m) of *Nicotiana obtusifolia*. (a-d) Expression of
808 *NiobALC* during floral organ development. (e, k) longitudinal section of a fruit during day 1-
809 2 after fertilization. (f-g, l-m) “intermediate” stages: day 3-4 after fertilization, but prior to
810 lignification of the endocarp. Arrowhead indicate the most distal part of the ovary in the site
811 connecting with the style and the stigma. Asterisks indicate seeds. b, bracts; fb, floral buds;
812 c, carpels; p, petals; pl, placenta; s, sepals; st, stamens; sp, septum. Scale bars= 50µm in
813 a,b,h,i; 100µm in c-g, j-m.

814 **Fig. 2** Expression analyses by *In situ* Hybridization of (a-f) *CaanALC* and (g-l) *CaanSPT* in
815 floral buds of *Capsicum annuum*. (a, g) early floral buds with forming sepals. (b, c, e, f, h, i,
816 k, l) longitudinal sections of floral buds at different developmental stages. (d, j) cross sections
817 of floral buds. s, sepals; p, petals; pl, placenta; o, ovules; st, stamens; c, carpels; fb, floral
818 buds; b, bract. Scale bars= 50µm in a,g; 100µm in b-f, h-l.

819 **Fig 3** Expression analyses by *In situ* Hybridization of (a-g) *SlyALC* and (h-n) *SlySPT* in
820 *Solanum lycopersicum*. (a-e; h-l) floral buds. (f; m) Fruits in longitudinal section at day 3
821 after fertilization. (g; n) Fruits in transverse section at day 8 after fertilization. Note that both
822 genes are detected in young fruits but only *SlyALC* is maintained at later stages. Arrow
823 indicates the distalmost part of the fruit. White arrowheads in j indicate the petal margins.
824 Black arrowhead indicates the inner-most layers of the fruit wall. Asterisks indicate seeds. s,
825 sepals; p, petals; st, stamens; c, carpels; o, ovules; sp, septum. Scale bars a, h, i, j= 50µm; b-
826 e; k, l= 100µm; f, g, m, n= 200µm.

827 **Fig. 4** Down-regulation of *ALC* and *SPT* genes in VIGS-treated plants. (a-c) RT-PCR using
828 cDNA prepared from leaves of VIGS-treated plants showing change in *ALC* and *SPT*
829 expression relative to wild-type leaves. For (a) *N. obtusifolia*, (b) *C. annuum* and (c) *S.*
830 *lycopersicum*. (d-e) Quantitative RT-PCR using cDNA prepared from leaves of VIGS-treated
831 plants that showed down-regulation of *ALC* and *SPT* in *C. annuum* (d) and *S. lycopersicum*
832 (e). *Niobalc/spt*, *Caanalc/spt* and *Slyalc/spt*: *ALC/SPT*-VIGS downregulated plants.
833 Numbers correspond to individuals screened with downregulation in the levels of both genes.

834 dm, double mutants. Values are means \pm SD for three technical replicates. *UBIQUITIN-3*
835 was used as the endogenous control.

836 **Fig. 5** Double *ALC/SPT-VIGS* down regulated *N. obtusifolia* plants with changes in flowers
837 and fruits development. (a-c) Wt and (d) *ALC/SPT-VIGS* flowers. (e) comparison of size of
838 florals organ between *ALC/SPT-VIGS* (right) and Wt (left). (f-h) Wt fruit phenotype, with
839 lignification during maturation restricted to two inner fruit wall layers (arrowhead in h). (i-
840 k) *ALC/SPT-VIGS* fruits start maturing earlier (arrows) with ectopic lignified patches in the
841 pericarp (arrowheads in k). (l-o) Phenotypes in the septum and placenta by SEM shown in
842 (l-m) Wt and (n-o) *ALC/SPT-VIGS* fruits. en, endocarp; ex, exocarp; me, mesocarp; p, petals;
843 pl, placenta; s, sepals; sp, septum. Scale bars a, f, g, i, j= 2mm; b-d = 5mm; l-o= 500 μ m.

844 **Fig. 6** Double *ALC/SPT-VIGS* down regulated *C. annuum* plants with changes in petal and
845 fruit development. (a-c) Wt flowers with posgenital petal fusion. (d-f) *ALC/SPT-VIGS*
846 flowers with premature exposure of stamens and carpel (d-e) and petal asymmetry during
847 anthesis (f). (g-j) Wt fruits. (k-n) *ALC/SPT-VIGS* fruits show lignified regions in the fruit
848 walls (arrows). Arrowhead indicate petal mutant. Asterisks indicate seeds. Stars indicate
849 giant endocarp cells that accumulate capsaicin. en, endocarp; ex, exocarp; me, mesocarp s,
850 sepals; p, petals; st, stamens; sp, septum. Scale bars a, b, d, e =0,5mm; c, f-i, k-m= 2mm.

851 **Fig. 7** Double *ALC/SPT-VIGS* down regulated *S. lycopersicum* plants with changes in petal
852 and fruit development. (a-d) Wt flowers with posgenital petal fusion. (e-h) *ALC/SPT-VIGS*
853 flowers with premature exposure of stamens and carpels (e,f) and petal asymmetry during
854 anthesis (g,h). (i-l) Wt fruits. (m-p) *ALC/SPT-VIGS* fruits show lignified regions in the fruit
855 walls (arrows). Arrowheads indicate smaller petals. Asterisks indicate seeds. fb, floral buds;
856 p, petals; pl, placenta; s, sepals; st, stamens; sp, septum. Scale bars a, b, e, f = 2mm; c, d, g,
857 h, i-p= 5mm

858 **Fig. 8** Double *ALC/SPT-VIGS* down regulated plants with change in leaf pigmentation. (a-
859 f) Wild type plants; (g-l) *ALC/SPT-VIGS* plants and (m-r) *PDS-VIGS* plants in (a, b, g, h, m,
860 n) *N. obtusifolia*, (c, d, i, j, o, p) *C. annuum* and (e, f, k, l, q, r) *S. lycopersicum*. The
861 spectrophotometric analyses on the abaxial side of all leaves photographed at the regions of
862 shifting pigmentation are shown in b, d, f, h, j, l, n, p, and r. Note the change in the reflectance
863 between 500-600nm the Wt and the *ALC/SPT-VIGS* down regulated plants. (b, d, f, h, j, l)

864 leaf phenotype. Arrows indicate places with changes in leaf pigmentation. Red, black and
865 blue colors in the curves represent three biological replicates of each species.

866 **Data Statement**

867 All sequences isolated and cloned during the experiments have been submitted to Genbank.
868 Alignments used are in the supplementary material. For plasmids, vectors and agrobacterium
869 strains a request should be made to Natalia Pabón-Mora at lucia.pabon@udea.edu.co

Figure 1

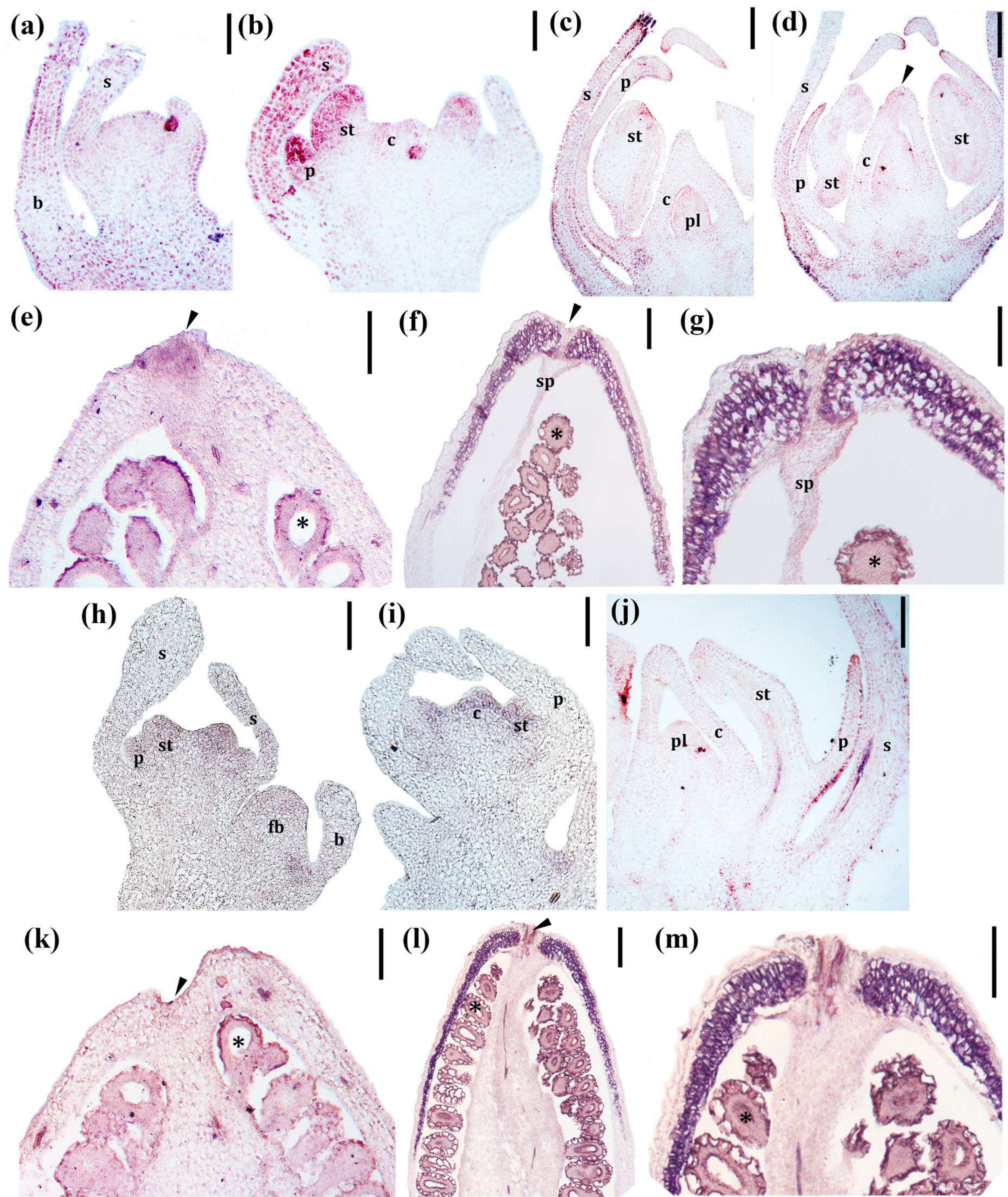
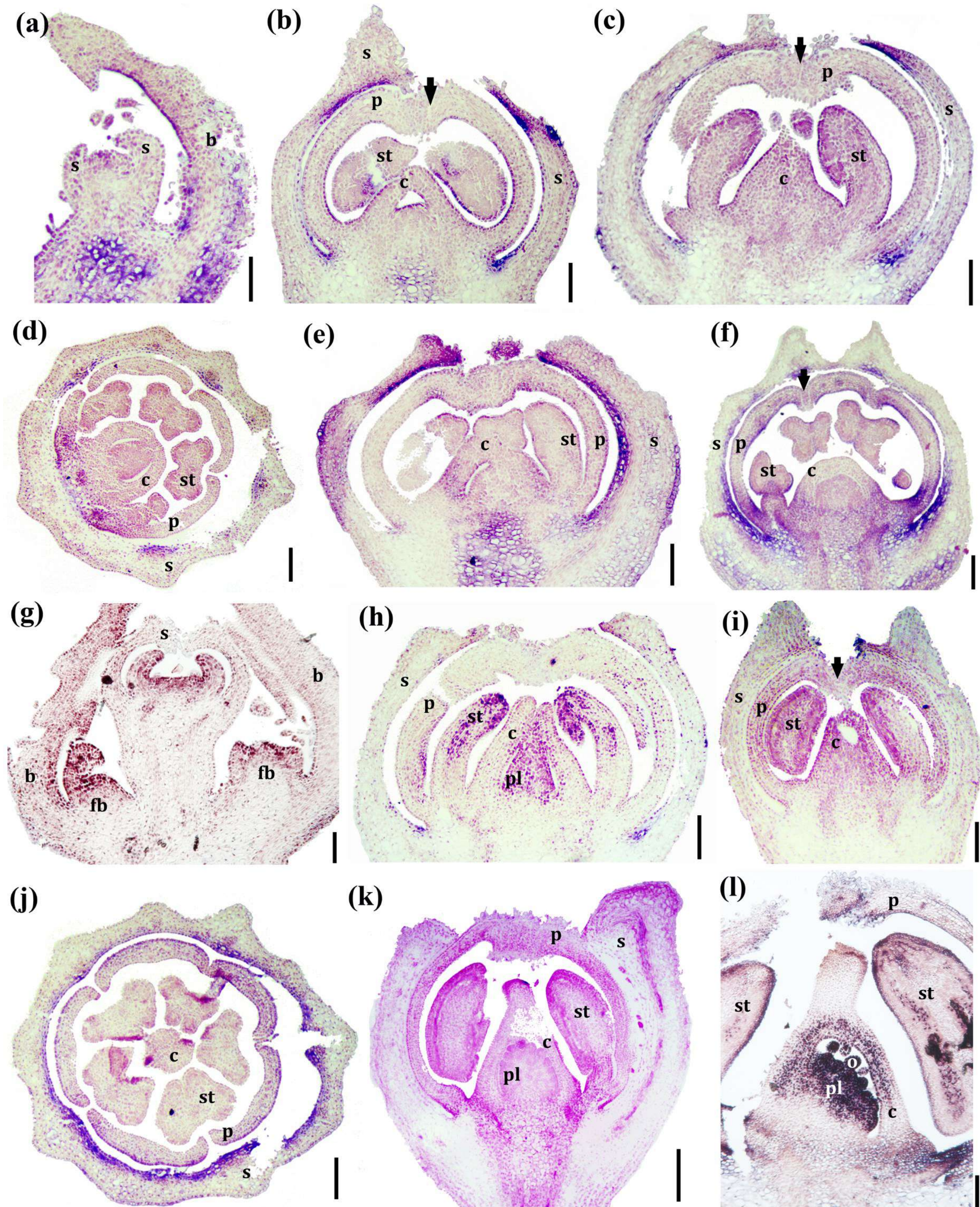
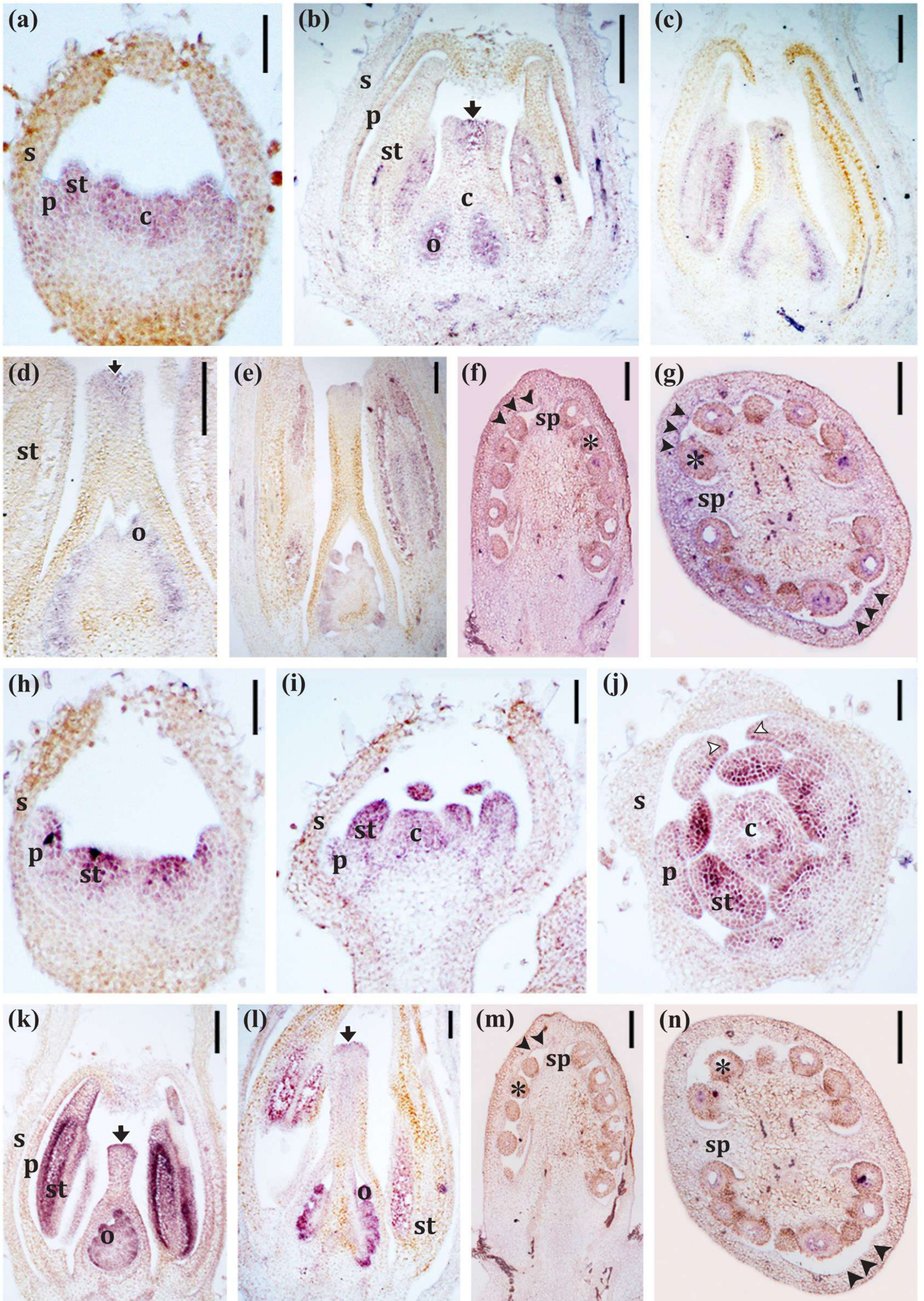
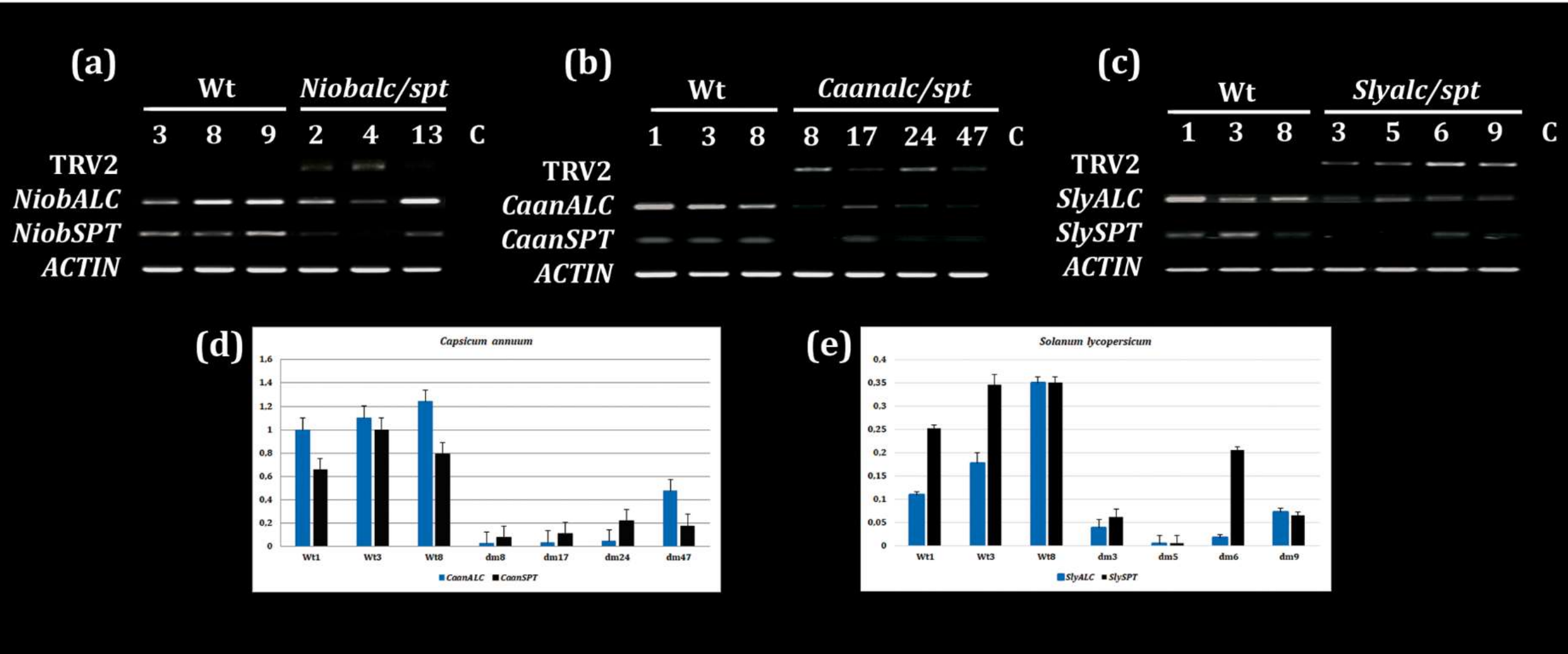


Figure 2







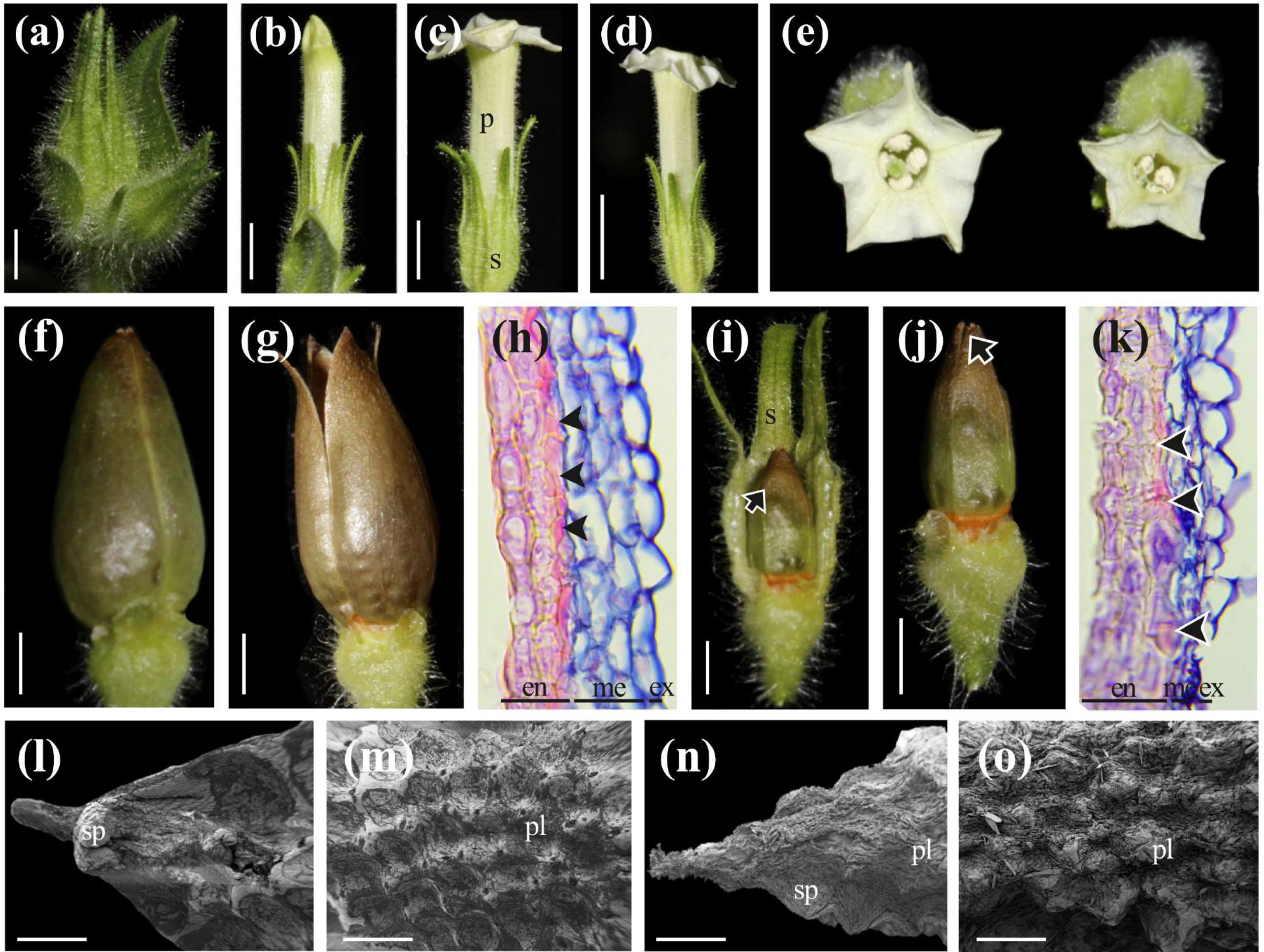
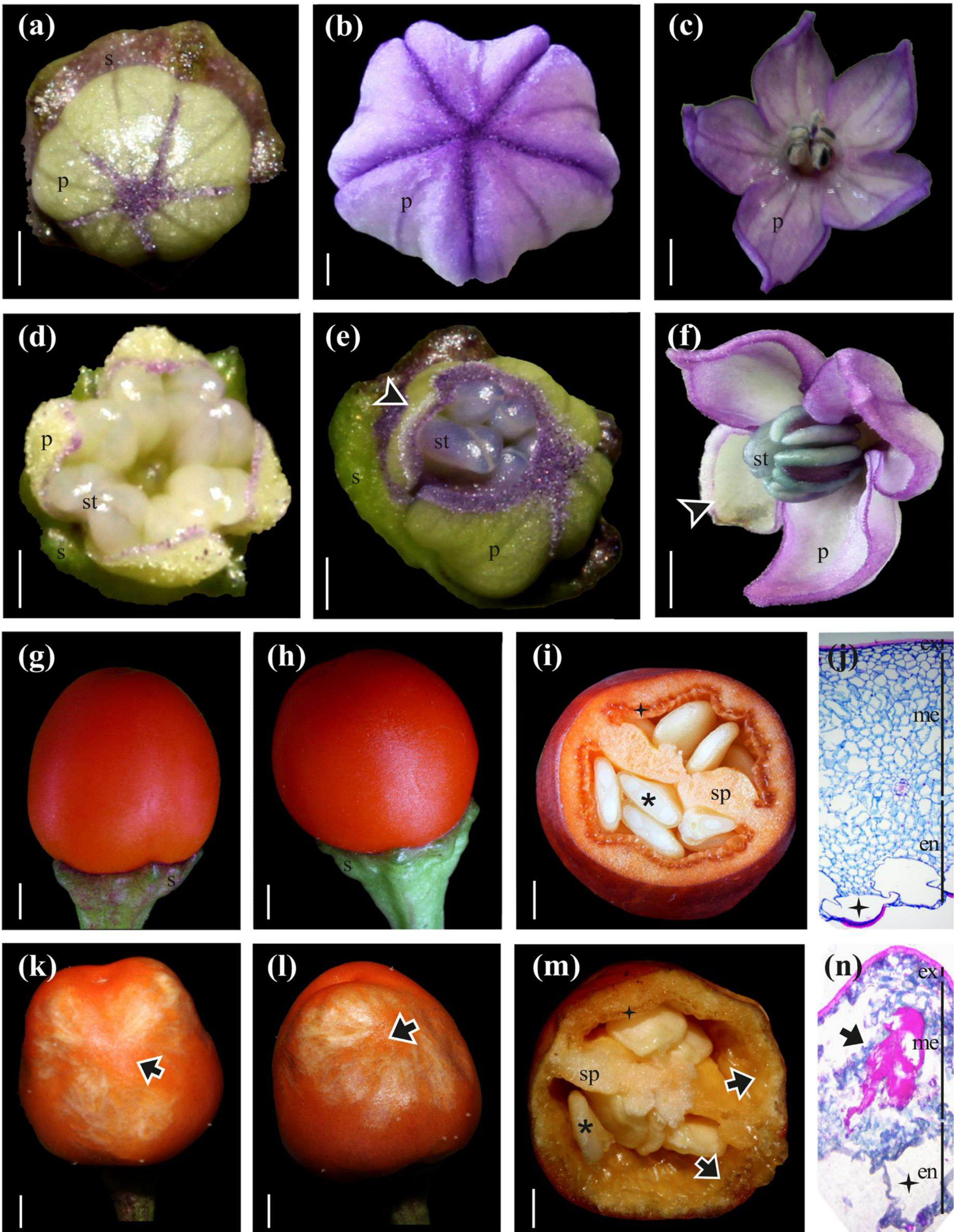
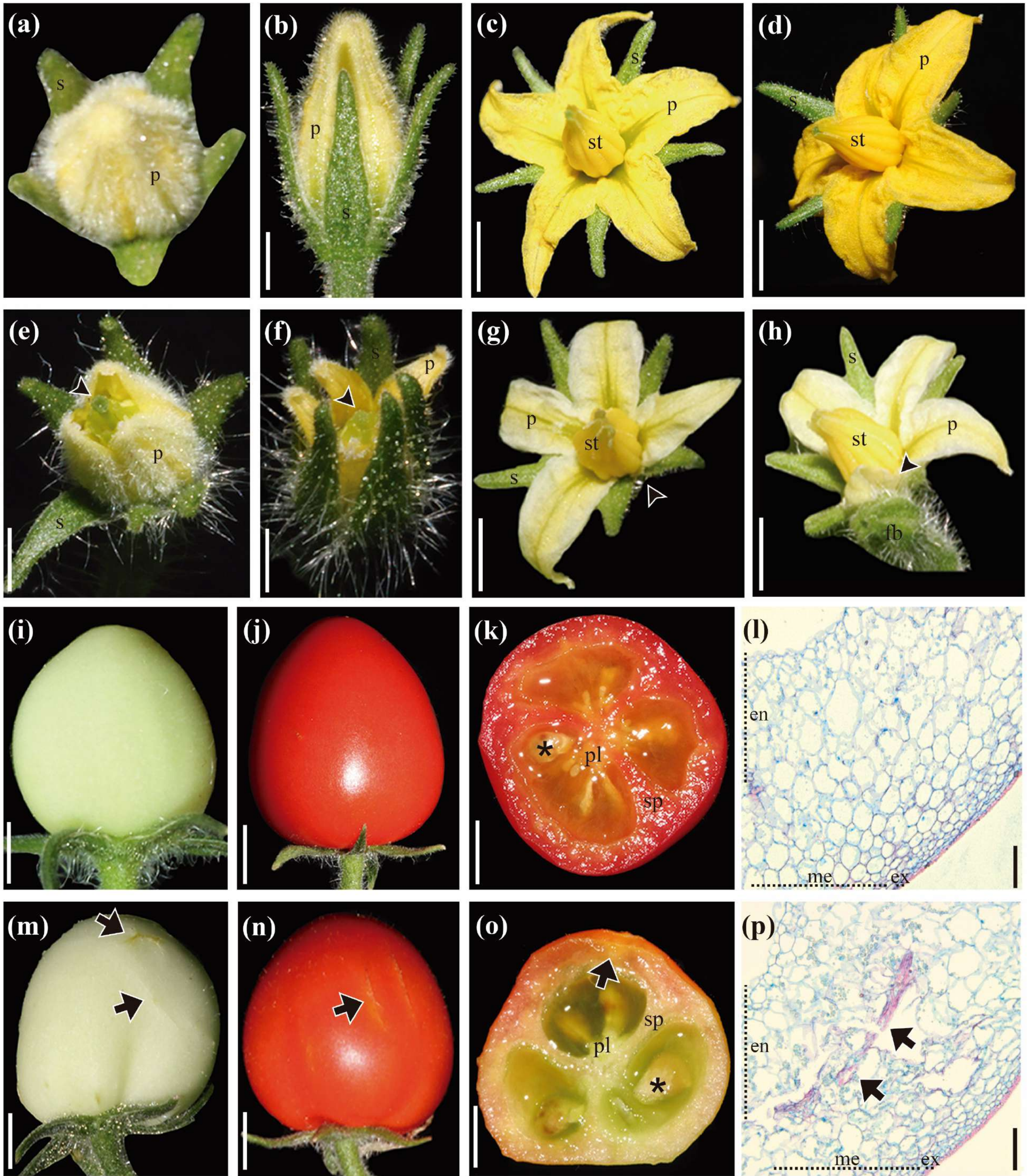


Figure 6



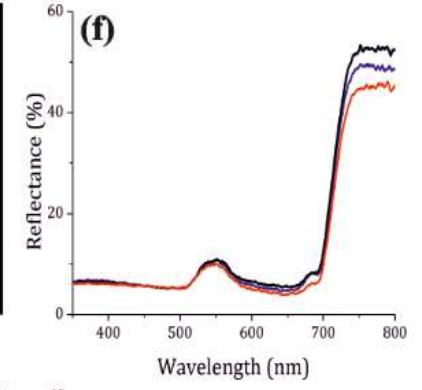
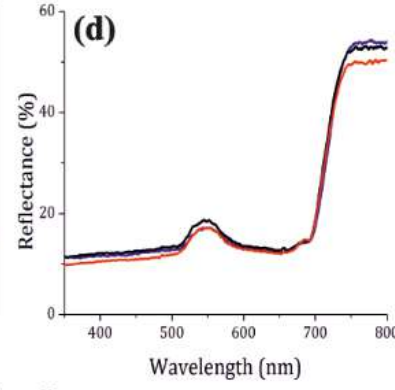
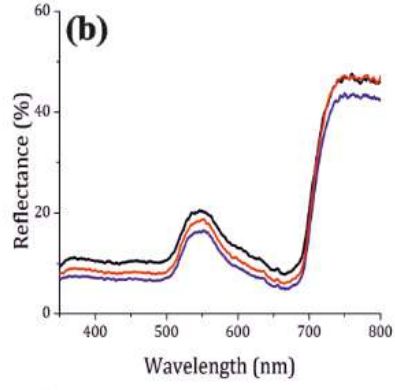
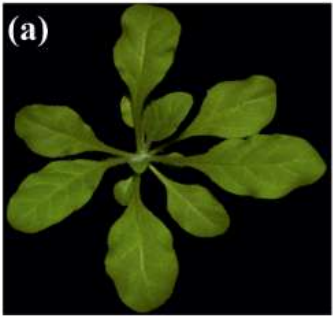


Nicotiana obtusifolia

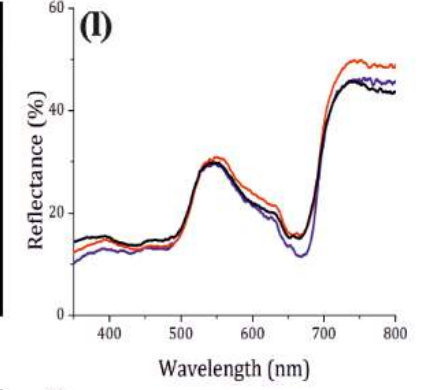
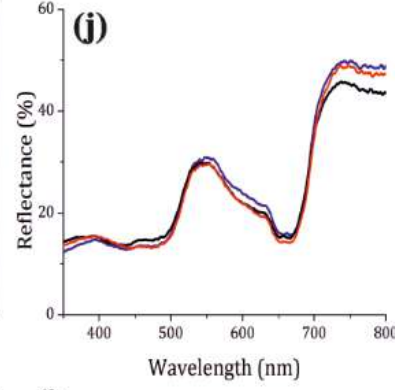
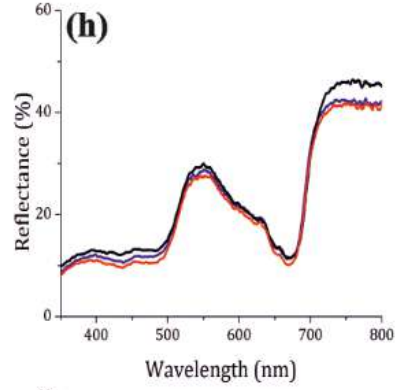
Capsicum annuum

Solanum lycopersicum

Wt



alc/spt



pds

